Characterization of B-type cyclins in the smut fungus *Ustilago maydis*: roles in morphogenesis and pathogenicity

Tatiana García-Muse[1], Gero Steinberg[2] and José Pérez-Martín[1,*]

[1]Department of Microbial Biotechnology, Centro Nacional de Biotecnología CSIC, Campus de Cantoblanco-UAM, 28049 Madrid, Spain
[2]Max-Planck-Institut für Terrestrische Mikrobiologie, Karl-von-Frisch-Strasse, 35043 Marburg, Germany
*Author for correspondence (e-mail: jperez@cnb.uam.es)

Accepted 17 September 2003
Journal of Cell Science 117, 487-506 Published by The Company of Biologists 2004
doi:10.1242/jcs.00877

Summary

Pathogenesis, morphogenesis and cell cycle are connected in the fungal pathogen *Ustilago maydis*. Here we report the characterization of the catalytic subunit of the cyclin-dependent kinase, encoded by the gene *cdk1*, and the two B-type cyclins present in this organism, encoded by the genes *clb1* and *clb2*. These cyclins are not redundant and appears to be essential for cell cycle. The analysis of conditional mutants in cyclin genes indicates that Clb1 is required for G1 to S and G2 to M transitions, while Clb2 is specifically required for the onset of mitosis. Both Clb1 and Clb2 carry functional destruction boxes, and expression of derivatives lacking D-boxes arrested cell cycle at a post-replicative stage. High levels of Clb1 generated cells with anomalous DNA content that were hypersensitive to microtubule-destabilizing drugs. In contrast, high levels of Clb2 induce premature entry into mitosis, suggesting that Clb2 is a mitotic inducer in *U. maydis*. In addition, Clb2 affects morphogenesis, and overexpression of *clb2* induces filamentous growth. Furthermore, we have found that appropriate levels of Clb2 cyclin are critical for a successful infection. Mutant strains with half a dose of *clb2* or high level of *clb2* expression are impaired at distinct stages in the infection process. These data reinforces the connections between cell cycle, morphogenesis and virulence in this smut fungus.

Key words: *Ustilago maydis*, Cell cycle, Cyclins, Cyclin-dependent kinase, Phytopathogenic fungus

Introduction

Ustilago maydis, a basidiomycete fungus, causes smut disease of maize. In this fungus, pathogenesis and sexual development are intricately interconnected, to the extent that *U. maydis* is completely dependent on the plant to accomplish a complete sexual cycle (Banuett, 1995). Haploid cells grow in yeast-like unicellular form, dividing by budding, and induction of the pathogenic phase requires the mating of two compatible haploid cells and the generation, after cell fusion, of an infective dikaryotic filament, which invades the plant (Kahmann et al., 2000). The transition from budding growth to mating is a response to environmental factors and the presence of compatible pheromone. In previous work, we demonstrated that mating is linked to cell cycle, and that cells of *U. maydis*, when exposed to pheromone, undergo a cell cycle arrest in G2 phase prior to mating (García-Muse et al., 2003). This cell cycle arrest contrasts with pheromone-induced cell cycle arrest in ascomycete yeasts such as *Saccharomyces cerevisiae* and *S. pombe*, which takes place in G1 phase (Sprague and Thorner, 1992; Davey, 1998), and suggests alternative mechanisms linking pheromone-response and cell cycle arrest in this basidiomycete fungus. To determine the mechanisms involved in pheromone-induced cell cycle arrest in *U. maydis*, we first found it necessary to make a careful study of the basic molecular components of cell cycle regulation, because so little information is available for this organism in this respect.

Previous studies related to cell cycle in *Ustilago maydis* have been focused on morphological descriptions of asynchronous cultures (O'Donnell and McLaughlin, 1984; Jacobs et al., 1994; Snetselaar and McCann, 1997; Steinberg et al., 2001; Banuett and Herskowitz, 2002). Vegetatively growing *U. maydis* cells normally produce one polar bud per cell cycle (Jacobs et al., 1994). Studies correlating nuclear density and cell morphology showed that cells complete DNA synthesis before beginning to form buds. In other words, the bud formation takes place in G2 phase (Snetselaar and McCann, 1997). This is in contrast to bud formation in *S. cerevisiae*, for example, which is reported to occur during S phase (Pringle and Hartwell, 1981). Once the bud is nearly mature, the nucleus migrates to the bud, where it divides (Holliday, 1974; O'Donnell and McLaughlin, 1984; Snetselaar, 1993; Banuett and Herskowitz, 2002). In rapidly growing cells, because cell division produces daughter cells with a mass similar to mother cells, G1 phase is very brief and the S phase begins shortly after cytokinesis. Therefore, cells have a 2C DNA content for most of the cell cycle (Snetselaar and McCann, 1997). Morphological studies of the cytoskeleton in dividing *U. maydis* cells have clearly defined the microtubule and actin organization during cell cycle, proving excellent markers of different cell cycle stages. For instance, *U. maydis* cells undergoing G2 phase assemble long microtubules towards the growth region while at the onset of mitosis, this network disassembles and is replaced by a spindle and prominent astral

Table 1. *Ustilago maydis* strains

Strain	Relevant genotype	Reference
FB1	*a1 b1*	Banuett and Herskowitz, 1989
FB2	*a2 b2*	Banuett and Herskowitz, 1989
FBD11	*a1 a2, b1 b2*	Banuett and Herskowitz, 1989
RWS2	*a1 b1*/ P_{otef}*cfp-tub1*, hyg^R	Wedlich-Söldner et al., 2002
TAU4	*a1 a2, b1 b2, cdk1 cdk1*Δ::*hph*, hyg^R	This study
TAU17	*a1 b1, cdk1-1*, hyg^R	This study
TAU26	*a1 b1, cbx*::P_{hsp70}*clb2-1*, cbx^R	This study
TAU30	*a1 b1, cbx*::P_{crg1}**clb1*Δ*db1*, cbx^R	This study
TAU31	*a1 b1, cbx*::P_{crg1}**clb1*Δ*db1-2*, cbx^R	This study
TAU36-1	*a1 b1, cbx*::P_{crg1}*clb1-1*, cbx^R	This study
TAU36-2	*a1 b1, cbx*::P_{crg1}**clb1-1*, cbx^R	This study
TAU41	*a1 b1, clb1*^{nar}, cbx^R	This study
TAU42	*a1 b1, clb2*^{nar}, cbx^R	This study
TAU45	*a1 b1, cbx*::P_{crg1}**clb1*Δ*db2*, cbx^R	This study
TAU52-1	*a1 b1, cbx*::P_{crg1}*clb2-1*, cbx^R	This study
TAU52-2	*a1 b1, cbx*::P_{crg1}**clb2-1*, cbx^R	This study
TAU53	*a1 b1, cbx*::P_{crg1}**clb2*Δ*db*, cbx^R	This study
TAU57	*a1 b1, cbx*::P_{crg1}**clb1*Δ*db1-2*, cbx^R/ P_{otef}*cfp-tub1*, hyg^R	This study
TAU58	*a1 b1, cbx*::P_{crg1}**clb2*Δ*db*, cbx^R/ P_{otef}*cfp-tub1*, hyg^R	This study
UMP19	*a1 b1, clb1-1*, hyg^R	This study
UMP21	*a1 a2, b1 b2, clb1 clb1*Δ*::hph*, hyg^R	This study
UMP25	*a1 b1, clb1*^{nar} cbx^R / P_{otef}*cfp-tub1*, hyg^R	This study
UMP26	*a1 b1, clb2*^{nar} cbx^R / P_{otef}*cfp-tub1*, hyg^R	This study
UMP27	*a1 b1, clb2-1*, hyg^R	This study
UMP32	*a1 a2, b1 b2, clb2 clb2*Δ*::cbx*, cbx^R	This study

a, b, mating type genes; P_{crg1}, arabinose-controled promoter; P_{crg1}*, less-active version of arabinose-controlled promoter; P_{hsp70}, constitutive promoter; P_{otef}, constitutive promoter; *clb1*^{nar} and *clb2*^{nar}, conditional ammonium-repressed alleles; *cfp-tub1*, cyan fluorescent protein-α tubulin fusion; /, ectopically integrated; hyg^R, hygromycin resistance; cbx^R, carboxine resistance.

microtubules (Steinberg et al., 2001; Banuett and Herskowitz, 2002).

In eukaryotes, major cell cycle controls regulate the onset of S phase and mitosis and ensure that these events occur in the correct sequence. Central to these controls are the cyclin-dependent kinases (CDKs), which are composed of a catalytic subunit and a regulatory subunit called cyclin. In fungi, a single catalytic subunit, encoded by *cdc2* in fission yeast and by *CDC28* in budding yeast, is required for both these cell cycle transitions (Krylov et al., 2003). Fungal Cdc2 homologues become associated with different cyclins that function during G1 for the onset of S phase and later in the cell cycle for the onset of mitosis (Nasmyth, 1993). In multicellular eukaryotes several catalytic subunits are present, which form a variety of complexes with different cyclins, regulating progression through the cell cycle (Nigg, 1995).

In an effort to characterize the molecular basis of the cell cycle regulation in *Ustilago maydis*, we have isolated the gene encoding the CDK catalytic subunit as well as the genes encoding the two B-cyclins of *U. maydis*. We have characterized the phenotypes of diverse gain-of-function and loss-of-function mutations in the cyclin genes in order to determine their function in mitosis and to distinguish any individual roles they may have. We show that these cyclins play a primary non-redundant role in different cell cycle events from S phase to progression through mitosis. Furthermore, we have found that the B-type cyclin Clb2 acts as a mitotic inducer in *U. maydis* and plays a fundamental role in morphogenesis and pathogenesis. We show that strains carrying anomalous *clb2* gene doses are affected in their cellular shape, and in the ability to successfully infect. To our knowledge this is the first report linking a cell cycle defect to virulence in a phytopathogenic fungus. The data reported in this work reinforce the postulated connections between cell cycle, morphogenesis and pathogenicity in *Ustilago maydis*.

Materials and Methods

Strains and growth conditions

For cloning purposes the *E. coli* K12 derivative DH5α (Bethesda Research Laboratories) was used. All *U. maydis* used in this study are listed in Table 1. Strains were grown at 28°C in yeast extract, peptone, dextrose medium (YPD), yeast extract, peptone, sucrose medium (YEPS) [modified after Tsukuda et al. (Tsukuda et al., 1988)], complete medium (CM) or minimal medium (MM) (Holliday, 1974). Conditional strains were grown in MM with nitrate (MM-NO_3) as the sole nitrogen source as described previously (Banks et al., 1993). To shut-off the P_{nar1} promoter, strains to be tested were grown in MM-NO_3 until OD_{600} of 0.2, pelleted by centrifugation, washed twice with minimal medium without nitrogen, and incubated in MM with ammonium as the nitrogen source (MM-NH_4) or YPD (Brachmann et al., 2001). For induction of the P_{crg1} promoter (Bottin et al., 1996; Brachmann et al., 2001), strains to be tested were grown in CM medium with 2% glucose as a carbon source (CMD) or rich medium (YPD) until OD_{600} of 0.2, pelleted by centrifugation, washed twice with water and incubated in CM with 2% arabinose (CMA) or rich medium with 2% arabinose (YPA). All chemicals used were of analytical grade and were obtained from Sigma or Merck.

Isolation of *cdk1* gene

Two sets of degenerate oligonucleotides were synthesized according to the nucleotide sequences that encode two conserved regions in CDK from different fungi: KLADFGLA (CDK1: 5′AARYTNGC-NGAYTTYGGNYTNGCN3′) and WYRAPE (CDK2a: 5′YTCNGG-NGCNCGRTACCA3′ and CDK2b: 5′YTCNGGNGCYCTRTA-

Table 2. Plasmids used in this study

Plasmid	Relevant allele	Marker	Integration site	Strains generated
pCDK-FLAG	*cdk1-1*	Hyg^R	*cdk1* locus	TAU17
pKOCDK	*cdk1Δ::hph*	Hyg^R	*cdk1* locus	TAU4
pCLB1-VSV	*clb1-1*	Hyg^R	*clb1* locus	UMP19
pKOCLB1	*clb1Δ::hph*	Hyg^R	*clb1* locus	UMP21
pCLB1nar	$clb1^{nar}$	Cbx^R	*clb1* locus	TAU41, UMP25
pRU11-CLB1	P_{crg1}*clb1-1*	Cbx^R	*cbx1* locus	TAU36-1
pRU12-CLB1	P_{crg1}**clb1-1*	Cbx^R	*cbx1* locus	TAU36-2
pRU12-CLB1Δdb1	P_{crg1}**clb1Δdb1*	Cbx^R	*cbx1* locus	TAU30
pRU12-CLB1Δdb2	P_{crg1}**clb1Δdb2*	Cbx^R	*cbx1* locus	TAU45
pRU12-CLB1Δdb1-2	P_{crg1}**clb1Δdb1-2*	Cbx^R	*cbx1* locus	TAU31, TAU57
pCLB2-MYC	*clb2-1*	Hyg^R	*clb2* locus	UMP27
pKOCLB2	*clb2Δ::cbx*	Cbx^R	*clb2* locus	UMP32
pCLB2nar	$clb2^{na}$	Cbx^R	*clb2* locus	TAU42, UMP26
pRU11-CLB2	P_{crg1}*clb2-1*	Cbx^R	*cbx1* locus	TAU52-1
pRU12-CLB2	P_{crg1}**clb2-1*	Cbx^R	*cbx1* locus	TAU52-2
pRU12-CLB2Δdb	P_{crg1}**clb2Δdb*	Cbx^R	*cbx1* locus	TAU53, TAU58
pCU1-CLB2	P_{hsp70}*clb2-1*	Cbx^R	*cbx1* locus	TAU26

CCA3′). The CDK1/CDK2a and CDK1/CDK2b pairs were used for amplification with 50 ng FBD11 DNA as template in a volume of 50 µl. PCR products were generated in the following reaction mixture: 10 mM Tris-HCl pH 8.0, 50 mM KCl, 1.2 mM $MgCl_2$, 100 µM dNTP, 50 µM of each primer and 2.5 units *Taq* polymerase. Conditions for PCR cycling included denaturation at 94°C for 1 minute, annealing at 45°C for 1 minute and extension at 72°C for 2 minutes. Selected fragments were isolated and cloned into pGEM-T Easy (Promega). Positive clones containing inserts were chosen and the nucleotide sequence of each plasmid insert was determined in both directions by the ABI model 373A Auto Sequence System (Perkin Elmer/Applied Biosystems). Three different kinds of inserts of the same size (93 bp) were obtained. The conceptual translation of these fragments generated amino acidic sequences with similarity to the sequence of CDK proteins from other fungi. Sequences flanking these fragments were obtained with a PCR-walking strategy (Siebert et al., 1995) using the Genome Walker system (Clontech) as directed by the manufacturer. The analysis of the sequence revealed three different ORFs: *cdk1*, which shows the highest similarity to *S. pombe* Cdc2, the main CDK in fission yeast (Beach et al., 1982); *cdk3*, which shows the highest sequence similarity to *S. cerevisiae* Srb10, a CDK involved in transcriptional regulation (Liao et al., 1995); and *crk1*, with the highest similarity to *S. cerevisiae* Ime2 (Garrido and Pérez-Martín, 2003).

Isolation of *clb1* and *clb2* genes

Two sets of degenerate oligonucleotides were synthesized according to the nucleotide sequences that encode two conserved regions in B-cyclins from different fungi: MVA/SEY (G2-1a: 5′ATGGTN-KCNGARTAY3′ and G2-1b: 5′ATGGTNAGYGARTAY3′) and FIAA/SKY (G2-2a: 5′TTYATHGCNKCNAARTAY3′ and G2-2b: 5′TTYATHGCNAGYAARTAY3′). Pairs of oligonucleotides were used for amplification with 50 ng FBD11 DNA as template as above. Two different kinds of inserts of the same size (282 bp) were obtained. The conceptual translation of these fragments generated amino acidic sequences with similarity to the sequence of B-type cyclins proteins from other fungi. Sequences flanking one of these fragments (the one encoding Clb1) were obtained with a PCR-walking strategy (Siebert et al., 1995) as above. Flanking sequences to the fragment encoding Clb2, were generously provided by Peter Schreier (Bayer CropScience AG, Monheim, Germany).

Plasmid constructions

Plasmids utilized in this study are listed in Table 2. Sequence analysis of fragments generated by PCR was performed with an automated sequencer (ABI 373A) and standard bioinformatic tools. Integration of the plasmids into the corresponding loci was verified in each case by diagnostic PCR and subsequent Southern blot analysis.

pCDK-FLAG

A fragment carrying the entire *cdk1* ORF sequence without stop codon and flanked by *Spe*I and *Eco*RI sites was obtained by amplification of genomic DNA with the primers CDK1 (5′GGACTAGTCATATGGACAAGTATCAAAGGATCGAA3′) and CDK4 (5′CGGAATTCTGTGAGGAGCCTCCTGAAGTACGG3′). This fragment was cloned in the pBS-FLAG-HYG plasmid digested with *Spe*I and *Eco*RI. The pBS-FLAG-HYG plasmid carries a copy of the FLAG epitope, and a hygromycin B resistance marker (J. P.-M., unpublished). After digestion with *Sac*II the pCDK-FLAG plasmid was integrated by homologous recombination into the *cdk1* locus.

pKOCDK

This plasmid was produced by ligation of a pair of DNA fragments flanking the *cdk1* ORF into pSMUT, a *U. maydis* integration vector containing a hygromycin B resistance cassette (Bölker et al., 1995) digested with *Bam*HI and *Xho*I. The 5′ fragment (flanked by *Bam*HI and *Not*I sites) spans from nucleotide –426 to nucleotide –18 (considering the adenine in the ATG as nucleotide +1) and it was produced by PCR amplification using the primers PCDK-A (5′ATTTGCGGCCGCTGGACAAACATCTTGGTCGGA3′) and PCDK-B (5′CGGGATCCAAGGGCAGGCGAAGAGCGACC3′). The 3′ fragment (flanked by *Not*I and *Xho*I sites) spans from nucleotide +740 to nucleotide +1094 and it was produced by PCR amplification using the primers TCDK-A (5′CCGCTCGAGCCCC-ACTGACGACGTTTGGCC3′) and TCDK-B (5′TAAAGCGGCC-GCGACGAGGCCAGCACGAAAAAA3′). After digestion with *Not*I the pKOCDK plasmid was integrated by homologous recombination into the *cdk1* locus.

pCLB1-VSV

A fragment carrying the entire *clb1* ORF sequence without stop codon and flanked by *Spe*I and *Eco*RI sites was obtained by amplification of genomic DNA with the primers ATGclb1 (5′GGACTAGTCATATGTCTCAGAACATCGTAAGCGCTC3′) and CLB-tag (5′CGGAATTCCTCCGTCGCTTCGTACGCGTT3′). This fragment was cloned in the plasmid pBS-VSV-HYG digested with *Spe*I and *Eco*RI. The plasmid pBS-VSV-HYG carries a copy of the VSV epitope and a hygromycin B resistance marker (J.P.-M.,

unpublished). After digestion with *Kpn*I the pCLB1-VSV plasmid was integrated by homologous recombination into the *clb1* locus.

pCLB2-MYC

A fragment carrying the entire *clb2* ORF sequence without stop codon and flanked by *Spe*I and *Eco*RI sites was obtained by amplification of genomic DNA with the primers CLB2-1 (5′GGACTAGT-CATATGCCACAACGCGCTGCCCTT3′) and CLB2-9 (5′CCGAA-TTCAGGCTGACCTGCTTGAGTCGA3′). This fragment was cloned in the plasmid pBS-MYC-HYG digested with *Spe*I and *Eco*RI The plasmid pBS-MYC-HYG carries three copies of MYC epitope and a hygromycin B resistance marker (J.P.-M., unpublished). After digestion with *Blp*I the pCLB2-MYC plasmid was integrated by homologous recombination into the *clb2* locus.

pKOCLB1

This plasmid was produced by ligation of a pair of DNA fragments flanking the *clb1* ORF into pNEBHyg(+), a *U. maydis* integration vector containing a hygromycin B resistance cassette (Brachmann et al., 2001) digested with *Eco*RI and *Sac*II. The 5′ fragment (flanked by *Eco*RI and *Kpn*I) was produced by PCR using the primers CYC1-2 (5′GGGGTACCTCGCGGTCATCGTACTAGACAG3′) and CYC1-3 (5′CAGCGCAAGCTGAGAATTCAACTTCCACTC3′). This fragment spans from nucleotide –1668 to nucleotide –894 (considering the adenine in the ATG as nucleotide +1). The 3′ fragment (flanked by *Kpn*I and *Sac*II) spans from nucleotide +2113 to nucleotide +2539 and it was produced by PCR amplification using the primers CYC1-7 (5′TCCCCGCGGAGACCTTCTAGATA-TCTTCCC3′) and CYC1-8 (5′CGGGGTACCCCAATCCGC-TTATGATTC3′). After digestion with *Kpn*I the pKOCLB1 plasmid was integrated by homologous recombination into the *clb1* locus.

pKOCLB2

This plasmid was produced by ligation of a pair of DNA fragments flanking the *clb2* ORF into pNEBCbx(+), a *U. maydis* integration vector containing a carboxine resistance cassette (Brachmann et al., 2001) digested with *Eco*RI and *Sac*II. The 5′ fragment (flanked by *Eco*RI and *Kpn*I) was produced by PCR using the primers CYC2-2 (5′CGGGGTACCTTTCTGCTATTGGCTTCAGCA3′) and CYC2-3 (5′CGGAATTCGGCTCGGAGTTTACTGCGGTAG3′). This fragment spans from nucleotide –498 to nucleotide –14 (considering the adenine in the ATG as nucleotide +1). The 3′ fragment (flanked by *Kpn*I and *Sac*II) spans from nucleotide +1753 to nucleotide +2278 and it was produced by PCR amplification using the primers CYC2-7 (5′TCCCCGCGGTCAATCTGAGAGGCACAGTTC3′) and CYC2-8 (5′CGGGGTACCTGGCTTTCGCACATCACATGG3′). After digestion with *Kpn*I the pKOCLB2 plasmid was integrated by homologous recombination into the *clb2* locus.

pCLB1nar

This plasmid was constructed by ligation of a pair of DNA fragments into pRU2, a *U. maydis* integration vector containing the promoter of the *nar1* gene (Brachmann et al., 2001) digested with *Nde*I and *Eco*RI. The 5′ fragment (flanked by *Eco*RI and *Kpn*I) was produced by PCR using the primers CYC1-2 and CYC1-3. The 3′ fragment (flanked by *Nde*I and *Kpn*I) was obtained by PCR amplification with primers ATGclb1 and CLB-tag and spans from nucleotide +1 to nucleotide +2114. After digestion with *Kpn*I the pCLB1nar plasmid was integrated by homologous recombination into the *clb1* locus.

pCLB2nar

This plasmid was constructed by ligation of a pair of DNA fragments into pRU2 digested with *Nde*I and *Eco*RI. The 5′ fragment (flanked by *Eco*RI and *Kpn*I) was produced by PCR using the primers CYC2-2 and CYC2-3. The 3′ fragment (flanked by *Nde*I and *Kpn*I) was obtained by PCR amplification with primers CLB2-1 and CYC2-6 (5′CGGGTACCTCCTCGGGATCGAGCCCCATGA3′) and spans from nucleotide +1 to nucleotide +773. After digestion with *Kpn*I the pCLB2nar plasmid was integrated by homologous recombination into the *clb2* locus.

Plasmids overexpressing *clb1*

The pRU11-CLB1 plasmid carries the VSV-tagged allele *clb1-1* cloned under the control of the P_{crg1} promoter. It was constructed by cloning a *Nde*I-*Afl*II fragment from pCLB1-VSV into the same sites of pRU11 (Brachmann et al., 2001). Plasmid pRU12-CLB1 was constructed in a similar way, but the pRU12 plasmid was used instead of pRU11. This plasmid carries a mutant version of the P_{crg1} promoter (that we called P_{crg1}*), which is around five times less active in the presence of arabinose than the P_{crg1} promoter present in pRU11 (Brachmann et al., 2001). The plasmids carrying Clb1 versions lacking the destruction boxes were constructed by exchanging the wild-type *clb1* ORF as a *Nde*I-*Eco*RI fragment from pRU12-CLB1 with fragments carrying the deleted versions obtained after PCR amplification with the following oligonucleotides: (i) pRU12-CLB1ΔDB1: ATG-Clb1 and CLB-dbTAG (5′CGGAATTCCTT-GACGCTGGGCAGCAGCCTT3′); (ii) pRU12-CLB1ΔDB2: CLB3 (5′GGACTAGTACTTTATGGAGATTTGCTCG3′) and CLB-TAG; (iii) pRU12-CLB1ΔDB1-2: CLB3 and CLB-dbATG. All of them were integrated after *Ssp*I linearization into the succinate dehydrogenase (*cbx*) locus as described previously (Brachmann et al., 2001).

Plasmids overexpressing *clb2*

The plasmid pRU11-CLB2 carries the MYC-tagged allele *clb2-1* cloned under the control of P_{crg1} promoter. It was constructed by cloning of a *Nde*I-*Afl*II fragment from pCLB2-MYC into the same sites of pRU11 (Brachmann et al., 2001). A similar construction was made by using the pRU12 plasmid, that carries the weaker P_{crg1}* promoter, giving the plasmid pRU12-CLB2. The derivative lacking the destruction box, pRU12-CLB2ΔDB was constructed by exchanging the wild-type *clb2* ORF as a *Nde*I-*Eco*RI fragment from pRU12-CLB2 with a fragment carrying the deleted version obtained after PCR amplification with the CLB2-2 (5′CGGGATCC-ATATGGTCGCCAGAGCCAATGCA3′) and CLB2-9 primers.

The pCU1-CLB2 plasmid expressing the *clb2-1* allele under the control of the constitutive P_{hsp70} promoter was constructing by cloning a *Nde*I-*Afl*II fragment from pCLB2-MYC into the same sites of pCU1 (Brachmann et al., 2001). All of them were integrated after linearization with *Ssp*I into the succinate dehydrogenase (*cbx*) locus.

Specific cell cycle arrests

Cell cycle arrests were carried out as described previously (García-Muse et al., 2003). To enrich the population in cells in G1 phase, a feed-starve regimen was followed as described previously (Holliday, 1965).

Protein analysis and kinase assay

For the preparation of crude protein extracts, cells were harvested by centrifugation at 4°C and washed twice with ice-cold water. The cell pellet was resuspended in ice-cold HB buffer (25 mM Mops pH 7.2, 15 mM $MgCl_2$, 15 mM EGTA, 1% Triton X-100, 20 μg/ml leupeptin, 40 μg/ml aprotinin, 0.1 mM sodium orthovanadate and 15 mM *p*-nitrophenyl phosphate). An equal volume of glass beads was added to this suspension and cells were broken by two bursts of vigorous vortexing for 3 minutes at 4°C. The glass beads and cell debris were

removed by centrifugation for 5 minutes in a microfuge. The supernatant was used for the different assays.

The affinity precipitation of Cdk1 was done by incubating 20 μl of Suc1-Sepharose beads (Calbiochem) with total protein extracts (50-150 μg) in HB buffer for 2 hours at 4°C with gentle agitation as described previously (Surana et al., 1993). The beads were then collected by centrifugation and washed six times with 1 ml of HB buffer.

For co-immunoprecipitation analysis, approximately 3.5 mg of total protein extracts were incubated with 1 μg of the monoclonal anti-myc 9E10 or anti-VSV-G (Roche Diagnostics Gmb) for 1 hour on ice, and then protein G-Sepharose beads (Pharmacia-Biotech) were added and incubated for 30 minutes at 4°C with agitation. Immunoprecipitates were washed six times with 1 ml of HB buffer.

For the kinase reaction, protein precipitates were incubated at 25°C for 10 minutes in KIN buffer (2 mg/ml histone H1, 200 μM [γ-^{32}P]ATP, 100 cpm/pmol in 25 mM Mops pH 7.2). The reaction was terminated by adding 5 μl of 5× Laemmli buffer, and then boiled for 3 minutes and loaded onto a 12.5% SDS-PAGE gel. Phosphorylated histone H1 was visualized by autoradiography.

Western analysis was performed on total protein extracts or the protein precipitates (50-100 μg), separated on 8-10% SDS-PAGE. Anti-PSTAIRE (Santa Cruz Biotechnology), anti-FLAG (M2; Kodak), anti-myc 9E10 (Roche Diagnostics Gmb) and anti-VSV-G (Roche Diagnostics GmbH) antibodies were used at 1:10000 dilution in phosphate-buffered saline +0.1% Tween + 10% dry milk. Anti-mouse-Ig-horseradish peroxidase and anti-rabbit-Ig-horseradish peroxidase (Roche Diagnostics Gmb) were used as a secondary antibody, at 1:10000 dilution. All western analyses were visualized using enhanced chemiluminescence (Renaissance®, Perkin Elmer).

RNA analysis

Total RNA was isolated as described previously (Garrido and Pérez-Martín, 2003). A 750 bp fragment spanning nucleotides +271 to +1021 (considering the adenine in the ATG as nucleotide +1) of the *clb1* gene and an 800 bp fragment that spans nucleotides +699 to +1499 of the *clb2* gene were used as a probe. A 5′-end labeled oligonucleotide complementary to the *U. maydis* 18S rRNA (Bottin et al., 1996) was used as loading control in northern analyses. A phosphorimager (Molecular Imager FX, Bio-Rad) and the program Quantity One (Bio-Rad) were used for visualization and quantification of radioactive signals.

Flow cytometry, light microscopy and image processing

Flow cytometry was performed as described previously (Garrido and Pérez-Martín, 2003). Nuclear staining was done using DAPI as described previously (Garrido and Pérez-Martín, 2003). WGA and calcofluor staining was performed as described previously (Wedlich-Söldner et al., 2000). Microscopy analysis was performed using a Zeiss Axiophot microscope. Frames were taken with a cooled CCD camera (Hamamatsu C4742-95). Epifluorescence was observed using standard FITC and DAPI filter sets. Cfp (cyan fluorescent protein) was analyzed with specific filter set (BP436, FT455, BP480-500). Image processing was performed with Image Pro Plus (Media Cibernetics) and Photoshop (Adobe).

Mating and plant infection

To test for mating, compatible strains were co-spotted on charcoal-containing PD plates (Holliday, 1974), which were sealed with Parafilm and incubated at 21°C for 48 hours.

Plant infections were performed as described previously (Gillissen et al., 1992) with the maize cultivar Early Golden bantam (Old Seeds, Madison, WI, USA). Filaments inside the plant tissue were stained with chlorazole black E as described previously (Brachmann et al., 2003).

Sequence analyses

Protein sequences of fungal CDKs and cyclins were downloaded from PubMed (http://www.ncbi.nlm.nih.gov/entrez/query.fcgi) and aligned in ClustalX (Thompson et al., 1997). Phylogenetic dendrograms were constructed using the minimal evolution method with a nearest neighbor joining tree as starting point and 500 Bootstrap replicates.

Results

The *cdk1* gene encodes the mitotic cyclin-dependent kinase in *U. maydis*

To identify genes encoding Cdc2 homologues in *U. maydis*, a PCR-based approach was adopted using degenerate primers that had been designed on the basis of conserved regions of CDK catalytic subunits from other fungi, as described in Materials and Methods. Three different PCR products were isolated and their sequences used to identify the full-length ORF by a PCR walking approach. After conceptual translation of the isolated ORFs, only one of the derived amino acid sequences showed the so-called PSTAIRE motif (Pines and Hunter, 1991) characteristic of functional Cdc2 homologues. The genomic sequence of this ORF was designated *cdk1* on the basis of the phenotypic characterization show below. It consisted of 1115 bp, which encoded a putative protein of 298 amino acids (accession number AY260971) with a calculated molecular mass of 34 kDa. Comparison of genomic and cDNA indicated that *cdk1* contains two introns of 121 bp and 100 bp length that are located 37 and 324 bp downstream of the start codon. Cdk1 shares 67% amino acid identity with Cdc2 from *S. pombe*, 66% with *S. cerevisiae* Cdc28, and 69% with *Candida albicans* Cdc28 (Fig. 1B). The Cdk1 protein contains all of the motifs characteristic of the Cdc2 homologues (Fig. 1A): (i) the above mentioned, PSTAIRE motif which has been implicated in the binding of the regulatory subunit, i.e. cyclin, to the CDK (Jeffrey et al., 1995); (ii) the specific threonine residue within the T-loop (at position 167 in *U. maydis* Cdk1) that is recognized by CDK-activating kinase (Fleig and Gould, 1991); (iii) the conserved tyrosine residue (Tyr 15) to be phosphorylated by the inhibitory Wee1 kinase (Fleig and Gould, 1991).

A cell lysate of a *U. maydis* wild-type strain separated by SDS-PAGE and probed with an anti-PSTAIRE antibody revealed the presence of two bands that migrated around 34-kDa (Fig. 1C). To determine which one of these cross-reactive band represented the Cdk1 protein, the chromosomal *cdk1* gene was replaced by the *cdk1-1* allele, which produces a Cdk1 protein that carries a copy of the FLAG epitope at the C terminus. An extract of the strain carrying the *cdk1-1* allele probed with an anti-PSTAIRE antibody showed that one of the bands shifted to a lower electrophoretic mobility (because of the size increase caused by the FLAG tag) with concomitant staining with the anti-FLAG antibody (Fig. 1C).

The *S. pombe* protein Suc1 is known to bind specifically to mitotic CDKs with high affinity (Ducommun and Beach, 1990). Consequently, Suc1 binding would provide a convenient assay for characterizing the *U. maydis* Cdk1 protein. Cell lysates from both a wild-type strain and the strain carrying the *cdk1-1* allele were then incubated with Suc1-conjugated Sepharose beads, and the precipitates were separated by SDS-PAGE followed by immunoblotting with anti-FLAG or anti-PSTAIRE antibodies (Fig. 1D). From total extracts, Suc1

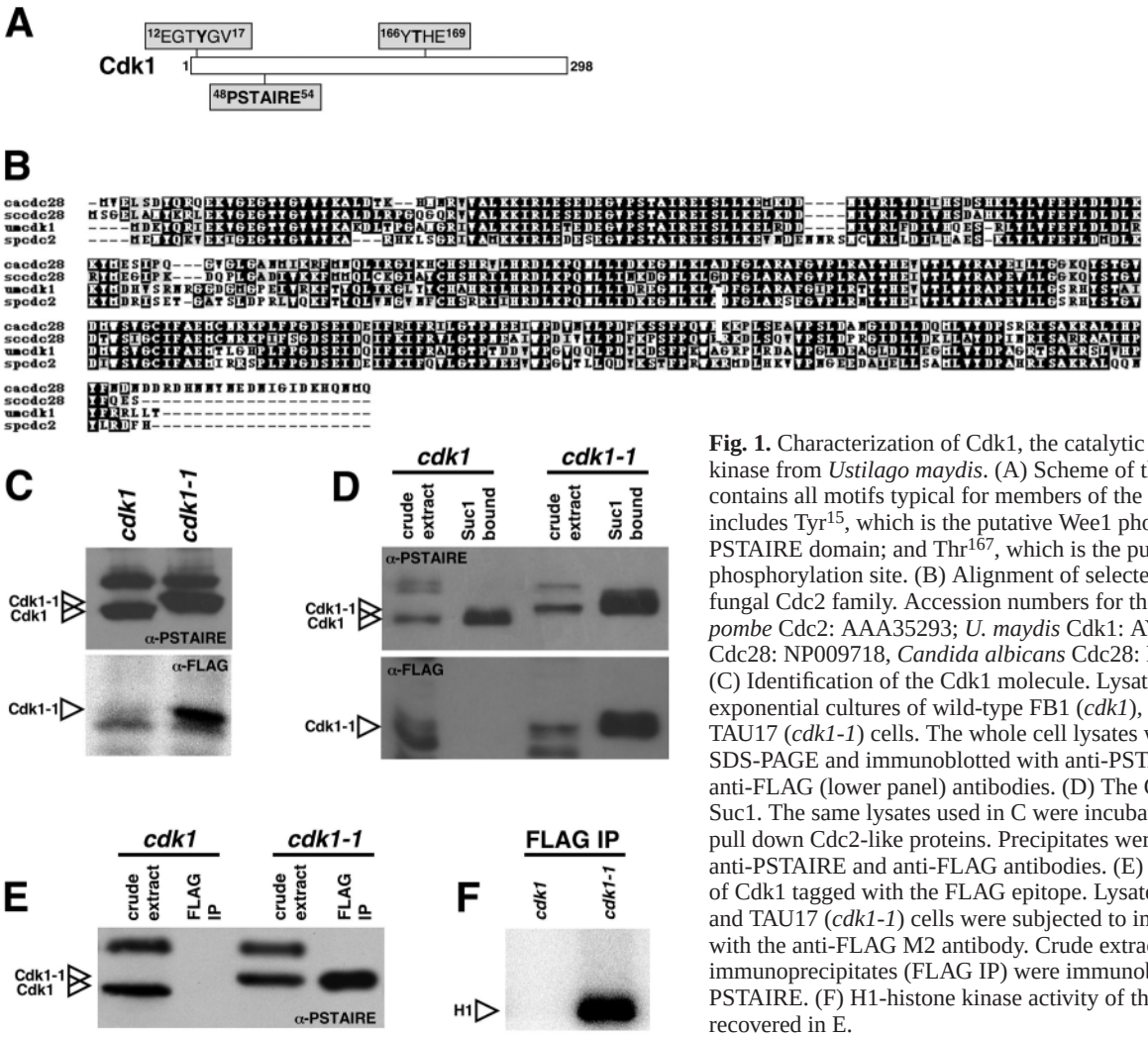

Fig. 1. Characterization of Cdk1, the catalytic subunit of the mitotic kinase from *Ustilago maydis*. (A) Scheme of the Cdk1 protein. Cdk1 contains all motifs typical for members of the Cdc2 family. This includes Tyr^{15}, which is the putative Wee1 phosphorylation site; a PSTAIRE domain; and Thr^{167}, which is the putative CAK phosphorylation site. (B) Alignment of selected members of the fungal Cdc2 family. Accession numbers for these proteins are: *S. pombe* Cdc2: AAA35293; *U. maydis* Cdk1: AY260971; *S. cerevisiae* Cdc28: NP009718, *Candida albicans* Cdc28: P43063. (C) Identification of the Cdk1 molecule. Lysates were prepared from exponential cultures of wild-type FB1 (*cdk1*), and tagged-strain TAU17 (*cdk1-1*) cells. The whole cell lysates were separated by SDS-PAGE and immunoblotted with anti-PSTAIRE (upper panel) or anti-FLAG (lower panel) antibodies. (D) The Cdk1 protein binds Suc1. The same lysates used in C were incubated with Suc1-beads to pull down Cdc2-like proteins. Precipitates were immunoblotted with anti-PSTAIRE and anti-FLAG antibodies. (E) Immunoprecipitation of Cdk1 tagged with the FLAG epitope. Lysates from FB1 (*cdk1*) and TAU17 (*cdk1-1*) cells were subjected to immunoprecipitation with the anti-FLAG M2 antibody. Crude extract or immunoprecipitates (FLAG IP) were immunoblotted with anti-PSTAIRE. (F) H1-histone kinase activity of the immunoprecipitates recovered in E.

precipitated only one of the two polypeptides recognized by the anti-PSTAIRE antibody, and in the tagged strain, the anti-FLAG antibody detected the Suc1-bound protein. Controls were made in which protein extracts of wild-type and tagged strains were incubated with Sepharose beads, in order to detect non-specific interaction between Cdk1 and the matrix. No Cdk1 was recovered in the bound fraction in these assays (not shown).

To determine the specific kinase activity associated with Cdk1, cell lysates of the tagged strain were then incubated with an anti-FLAG M2 affinity gel and the immunoprecipitates were analyzed by western blot assays with anti-PSTAIRE antibodies (Fig. 1E) or assayed for histone H1 kinase activity (Fig. 1F). Cell lysates from the wild-type strain were used as a negative control. The precipitated complex was able to phosphorylate histone H1 quite efficiently, while the negative control showed no kinase activity (Fig. 1F). The kinase activity correlates with the presence of a band detected by the anti-PSTAIRE antibody in the immunoprecipitate (Fig. 1E).

These lines of evidence strongly suggest that the Suc1-associated, and anti-PSTAIRE-recognized 34-kDa protein is likely to be the catalytic subunit of the *U. maydis* mitotic CDK. To prove that indeed the *cdk1* gene encodes a protein essential to growth, we inactivated one of the two *cdk1* alleles by replacement with a hygromycin B resistance cassette (giving the *cdk1*Δ::*hph* null allele) in the diploid strain FBD11, and after sporulation we analyzed the meiotic progeny. No viable haploid hygromycin B resistant cells were obtained in the meiotic products indicating that the *cdk1* gene encodes an essential mitotic CDK in *U. maydis*.

The *clb1* and *clb2* genes encode B-type cyclins

To isolate genes encoding B-type cyclins from *U. maydis*, a degenerate PCR approach using oligonucleotide primers corresponding to conserved regions of fungal B-type cyclins was utilized. Two different fragments were recovered, and the respective full-length genes were isolated as described in Materials and Methods. The genomic sequences of these ORFs were designated *clb1* and *clb2*, and they encoded putative proteins of 707 and 539 amino acids respectively (accession numbers AY260969 and AY260970). Comparison of genomic DNA and cDNA indicated that both genes were intronless (not shown). The conceptual translation of *clb1* and *clb2*, indicated that the predicted proteins contained typical motives shared among all members of the B-type cyclin family, such as the

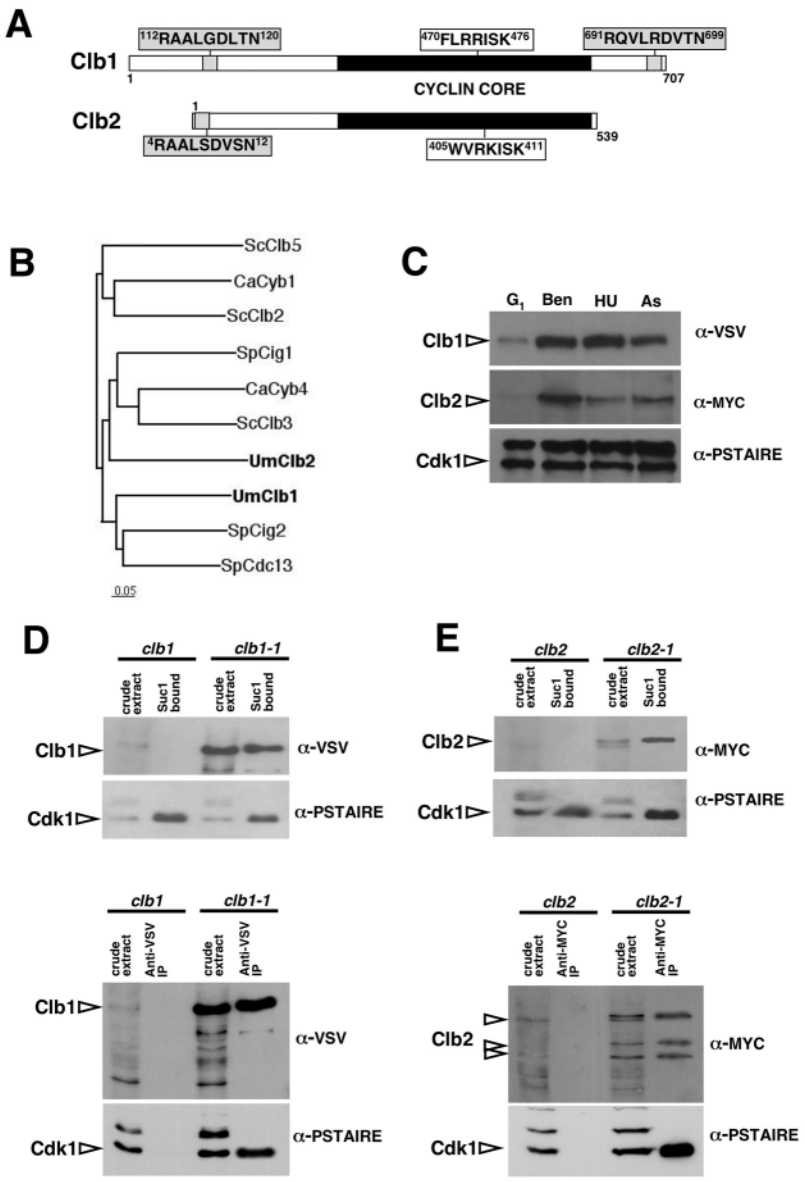

Fig. 2. Characterization of B-type cyclins from *U. maydis*. (A) Scheme of Clb1 and Clb2 proteins. *U. maydis* cyclins contained the FLRRXSK motif (white boxes) and 'destruction box' consensus sequences (gray boxes). (B) Dendrogram of selected B-type cyclins from fungi. *U. maydis* Clb1 groups with the S- and M-phase cyclins from *S. pombe*, while *U. maydis* Clb2 groups with a heterogeneous B-type cyclins. Accession numbers for the proteins are: ScClb5, P30283; CaCyb1, U40430; ScClb2, S14166; SpCig1, P24865; CaCyb4, AAC79857; ScClb3, A60048; UmClb2, AY260970; UmClb1, AY260969; SpCig2, P36630; SpCdc13, P10815. Bar: 0,05 substitutions per aa. (C) Clb1 and Clb2 are highly abundant in S- and G2/M-arrested cells, but present at low levels in G1 cells. Extracts from cells carrying an epitope-tagged copy of Clb1 and Clb2 were analyzed by immunoblotting. Samples are as follows: G_1, culture enriched in G1 phase cells; Ben, cells arrested at G2/M transition after treatment with benomyl for 1 hour; HU, cells arrested in S phase by treatment with hydroxyurea for 90 minutes; As, asynchronous cells. The same filters were also probed with anti-PSTAIRE antibodies (bottom panel), showing that the abundance of Cdk1 varied less than twofold. (D) Clb1 associates with Cdk1. Lysates prepared from wild-type FB1 and Clb1-tagged UMP19 (*clb1-1*) cells were incubated with Suc1 beads to pull down Cdk1 (upper panel) or were immunoprecipitated with anti-VSV antibody to pull down Clb1 (lower panel). The whole cell lysates as well as the precipitates were separated by SDS-PAGE and immunoblotted with anti-PSTAIRE and anti-VSV to detect Cdk1 and Clb1 proteins respectively. (E) Clb2 associates with Cdk1. Lysates prepared from wild-type FB1 and Clb2-tagged UMP27 (*clb2-1*) cells were incubated with Suc1 beads to pull down Cdk1 (upper panel) or were immunoprecipitated with anti-MYC antibody to pull down Clb2 (lower panel). The whole cell lysates, as well as the precipitates, were separated by SDS-PAGE and immunoblotted with anti-PSTAIRE and anti-MYC to detect Cdk1 and Clb2 proteins respectively. The different bands with higher electrophoretic mobility detected in the anti-MYC IP are degradation products of Clb2.

FLRRXSK motif-less conserved in Clb2- (Fitch et al., 1992) and the 'destruction box' motif, which is involved in the degradation of cyclins mediated by the APC/cyclosome (Glotzer et al., 1991) (Fig. 2A). Sequence comparison indicates an overall 30% sequence identity between *U. maydis* cyclins and B-type cyclins from other fungi (not shown). A dendrogram analysis (Fig. 2B) indicates that the two *U. maydis* proteins fall in two different branches. In one branch, *U. maydis* Clb1 is grouped along with the *S. pombe* cyclins Cig2 and Cdc13, which are involved in the G1 to S and G2 to M transitions, respectively (Fisher and Nurse, 1995). The second branch grouped *U. maydis* Clb2 protein with the *S. cerevisiae* Clb3, the *S. pombe* Cig1 and *C. albicans* Cyb4 proteins. From these cyclins only a clear role has been assigned to Clb3, which is a G2/M phase cyclin (Fitch et al., 1992; Richardson et al., 1992).

For *clb1* and *clb2* to qualify as the genes encoding true B-type cyclins, their protein products must fulfill at least two criteria: they must associate with the catalytic subunit Cdk1 to form the mitotic CDK, and their levels must fluctuate during the cell cycle, falling as cells enter G1 and rising again as cells enter S/G2/M. To examine these requisites, we exchanged the chromosomal locus of *clb1* and *clb2* with the functional *clb1-1* and *clb2-1* alleles, encoding VSV- and MYC-tagged versions of Clb1 and Clb2, respectively. To determine whether the levels of Clb1 and Clb2 fluctuate through the cell cycle, because no reproducible synchronization method is available so far in *U. maydis*, we used cell cultures arrested in different cell cycle stages. Protein extracts were prepared from cultures of the tagged strains enriched in G1 phase or arrested in the presence of hydroxyurea (S phase) and benomyl (G2/M phase). Clb1 and Clb2 protein levels were measured by western blotting with the use of anti-VSV and anti-MYC antibodies (Fig. 2C). Low amounts of Clb1 and Clb2 proteins were detected in cells enriched in G1 phase, while they were clearly present in cells arrested either in S phase or G2/M phase.

To show a physical association between the B-type cyclins and Cdk1, we used a double approach. Firstly, cell lysates of the tagged strains were incubated with Suc1-beads that bind

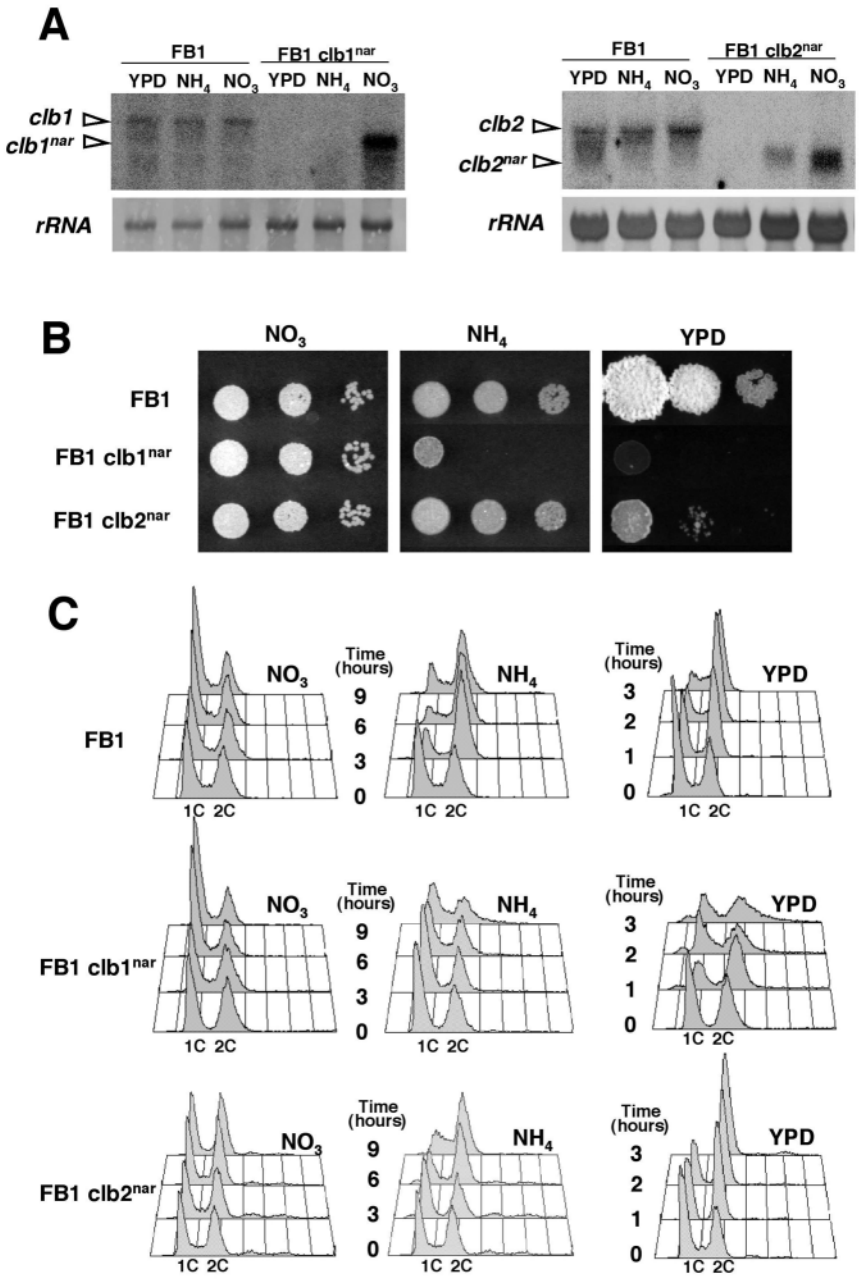

Fig. 3. Conditional removal of cyclins. (A) Levels of *clb1* and *clb2* mRNA in the conditional strains. Wild-type FB1 and conditional strains TAU41 (FB1 clb1^{nar}) and TAU42 (FB1 clb2^{nar}) were grown for 3 hours in permissive conditions [minimal medium with nitrate (NO_3)] or restrictive conditions [minimal medium with ammonium (NH_4), or rich medium, (YPD)] and then RNA was extracted and subjected to northern analysis, after loading 10 μg total RNA per lane. The filters were hybridized with probes for *clb1* or *clb2*. A probe for 18s rRNA was used as loading control. (B) Growth of conditional strain in solid medium. Serial tenfold dilutions of FB1, TAU41 (FB1 clb1^{nar}) and TAU42 (FB1 clb2^{nar}) cultures were spotted on solid rich medium (YPD), and minimal medium amended with nitrate (NO_3) or ammonium (NH_4). YPD and ammonium plates were incubated for 2 days, while nitrate plates were incubated for 3 days. All incubations were at 28°C. (C) Flow cytometry analysis of wild-type, TAU41 and TAU42 cells grown in permissive and restrictive conditions. Cells grown in MM-NO_3 were centrifuged, washed twice in minimal medium without nitrogen, and resuspended in the appropriated medium. Samples were taken for FACS analysis at the indicated times. Because of the shorter generation time of cells in rich medium, samples were taken every hour for a total of 3 hours.

specifically to CDKs, and the precipitates were separated by SDS-PAGE followed by immunoblotting with anti-VSV and anti-MYC antibodies. As shown in Fig. 2D,E (upper panels), both Clb1 and Clb2 were recovered in the fraction of proteins bound to Suc1-beads. Secondly, protein extracts from both tagged and wild-type cells were prepared, and VSV- and MYC-tagged proteins were immunoprecipitated and analysed for the presence of Cdk1 (Fig. 2D,E, lower panels). High levels of Cdk1 co-precipitated with Clb1-VSV and Clb2-MYC, while none was detected in precipitates of untagged extracts. Taken together, these results indicate that the *clb1* and *clb2* genes encode B-type cyclins in *U. maydis*.

Conditional removal of cyclin function

We tried unsuccessfully to delete the *clb1* and *clb2* genes in haploid cells, whilst we were successful in the removal of a single copy of each gene in diploid strains (not shown). Since these results strongly suggest that *clb1* and *clb2* represent essential genes, we constructed strains in which the cyclin function could be conditionally controlled. To achieve conditional expression of cyclin genes, the *U. maydis* P_{nar1} promoter, which is induced by nitrate and repressed by ammonium (Banks et al., 1993; Brachmann et al., 2001), was used. Two chimeric alleles were constructed composed of the P_{nar1} promoter fused to the coding region of *clb1* (*clb1^{nar}*) and the coding region of *clb2* (*clb2^{nar}*). In both cases, the respective native allele was replaced by the conditional allele.

In the *clb1* conditional strain, TAU41, the *clb1* mRNA was elevated around tenfold with respect to wild-type in minimal medium containing nitrate (MM-NO_3), and it was not detectable in minimal medium supplemented with ammonium (MM-NH_4) and rich medium YPD (Fig. 3A). TAU41 cells grew on solid minimal medium containing nitrate at a rate similar to control wild-type cells, but they were unable to form colonies when shifted to solid minimal medium containing ammonium or YPD (Fig. 3B), indicating an essential role of the Clb1 function.

In the *clb2* conditional strain, TAU42, the *clb2* mRNA was elevated around fourfold with respect to wild-type in permissive conditions (MM-NO_3), whereas it was decreased fivefold in MM supplemented with ammonium (MM-NH_4) and

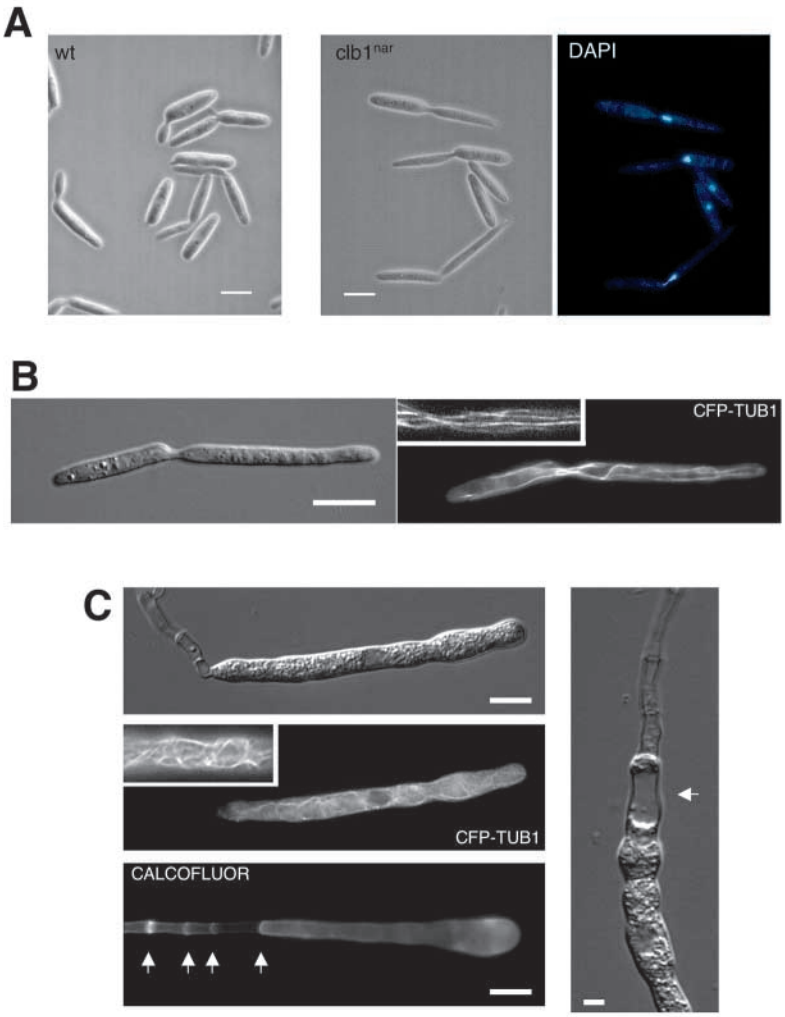

Fig. 4. Morphology of *clb1* conditional cells. (A) Morphology of the wild-type and mutant cells in restrictive conditions. FB1 and UMP25 cells were incubated for 9 hours in MM-NH_4. Two clear morphologies can be seen: unbudded and budded cells, all of them with a single nucleus per cell (right panel shows DNA stained with DAPI). Scale bar: 10 μm. (B) Microtubule organization in UMP25 cell arrested after 6 hours in rich medium. Note that in arrested cells long microtubules reach from the neck to the growing tip. (C) UMP25 cells incubated for 25 hours in rich medium have a distinct phenotype characterized by a extensive polarized growth (upper horizontal panel) disorganized tubulin cytoskeleton (middle horizontal panel) and empty sections behind that are separated by septa (stained with calcofluor in lower horizontal panel, arrows point the septa) generated by formation of basal vacuoles (arrow; vertical panel). Scale bars: (horizontal panels) 10 μm; (vertical panel) 5 μm.

it was barely detectable in YPD medium (Fig. 3A). Consistent with this pattern of expression, the *clb2* conditional strain showed no difference in colony growth with respect to a wild-type strain in minimal medium containing nitrate or ammonium, and was clearly defective in growth in YPD medium (Fig. 3B). The differences of transcriptional repression in non-permissive conditions between the *clb1* and *clb2* conditional alleles could be explained by the different tightness in the control of the P_{nar} promoter depending on the chromosomal context (our unpublished observations).

We analyzed the growth of the conditional strains in liquid medium by following the duplication time (by measuring the colony forming unit increase) and DNA content (by FACS analysis) of the cells during at least three generations after transfer from conditional medium (MM-NO_3) to tester medium. *U. maydis* FB1 cells had a duplication time of 260, 210 and 90 minutes growing in MM-NO_3, MM-NH_4 and YPD, respectively. More than 80% of the wild-type cells growing in MM-NO_3 had a 1C DNA content, indicating that they were passing through G1 phase. In MM-NH_4 medium, this proportion decreased to less than 40% and in rich medium it was only around 10% of the cells (Fig. 3C).

For TAU41 strain, we observed that in permissive conditions (MM-NO_3) the duplication time and DNA content profile of the population was similar to the wild-type strain. However, the cells stop dividing in approximately two generations after the transfer to restrictive conditions (MM-NH_4 or YPD). This cell duplication arrest is concomitant with the accumulation of cells, of which approx. 50% have 1C and 50% have 2C DNA content (Fig. 3C).

The *clb2* conditional cells growing in MM-NO_3 had a slight decrease in the duplication time (around 240 minutes) and the proportion of cells passing through G1 decreases to 50% of the population. No differences were apparent in cells growing in MM-NH_4, while after the transfer of cultures to rich medium, the cells stop dividing in three generations, with the cell population having a 2C DNA content (Fig. 3C).

Clb1 is required to enter in S and M phase

The DNA content analysis of the arrested *clb1* conditional strain suggested that Clb1 is required at different cell cycle stages. To characterize the phenotype of conditional cells, we introduced the *clb1* conditional allele in a FB1 strain carrying a Cfp-α tubulin fusion (Wedlich-Söldner et al., 2002), generating the UMP25 strain which showed all the previously described phenotypes of the conditional TAU41 strain (not shown). UMP25 cells incubated in permissive conditions for 9 hours were morphologically wild type (not shown). However, after 6 hours of incubation in restrictive conditions (rich medium), the conditional strain arrested with the cells showing two alternative morphologies (Fig. 4A): around 47% of the cell population was composed of unbudded cells, while the rest of the cells showed a developed bud that frequently (25% of total cells) was larger than the mother cell. In contrast, in wild-type cells growing in the same conditions, different stages of bud formation can be found (Fig. 4A, left panel). All arrested conditional cells contained a single nucleus (Fig. 4A). Measurement of the relative fluorescence of the nuclei by microphotometric methods (Snetselaar and McCann, 1997) indicated that fluorescence in budded cells were usually about twice as intense as that in unbudded cells (not shown). These data strongly suggest that Clb1 depletion resulted in a cell cycle arrest at two different points: a pre-replicative arrest (unbudded

cells with 1C DNA content) and a post-replicative arrest (budded cells with 2C DNA content). Of note, in budded arrested cells, the nucleus could be found either in the mother, neck or bud compartments (Fig. 4A). Because in *U. maydis* there is a migration of the nucleus to the bud compartment prior to mitosis (Holliday, 1974; O'Donnell and McLaughlin, 1984; Snetselaar, 1993; Banuett and Herskowitz, 2002), we investigated the organization of microtubules to define which kind of post-replicative arrest is taking place after Clb1 depletion. In *U. maydis* the microtubule cytoskeleton changes from a G2 cytoplasmic array, which is characterized by three to four bundles of microtubules that point towards the growth region, to a mitotic spindle that elongates after the metaphase-anaphase transition (Steinberg et al., 2001; Banuett and Herskowitz, 2002). After shift to restrictive conditions, conditional cells that made large buds contained long microtubules bundles that extend to the apical growth region (Fig. 4B), supporting a G2 arrest. Taking together all these lines of evidence, we conclude that Clb1 is required both for G1 to S and G2 to M transitions.

In the course of these experiments, we observed that more than 24 hours incubation of conditional cells in rich medium resulted in a bizarre phenotype consisting of large polarized cells (more than 60 μm in length), with an altered MT cytoskeleton, which formed basal vacuoles and had, posteriorly, empty sections that were separated by septa (Fig. 4C). Although we have no clear explanation for this behavior, we suspect that this could be the usual response in *U. maydis* to a continuous polar growth in a situation of arrested cell division. For instance, these cells are reminiscent of the growth mode of the dikaryotic hyphae produced after a successful mating, conditions in which a cell division arrest and a permanent polarized growth are present (Steinberg et al., 1998).

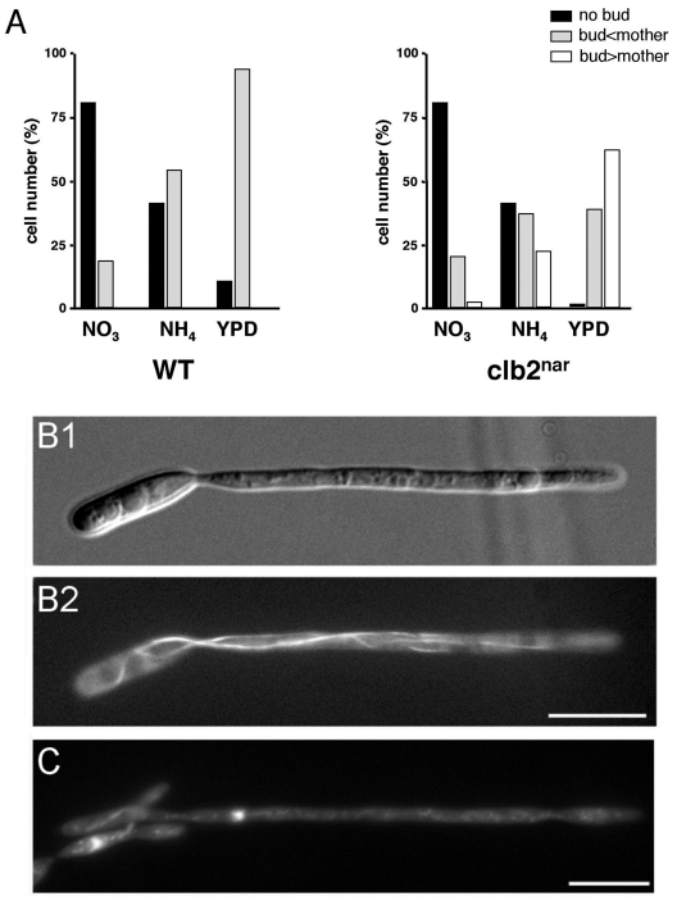

Fig. 5. Morphology of *clb2* conditional cells. (A) Quantification of FB1 (WT) and UMP26 (clb2^{nar}) cells growing in different media showing the proportion of unbudded cells, cells with a bud shorter than the mother cell and cells with a bud larger than the mother cell. More than 100 cells were recorded in each condition. (B) UMP26 cells were grown in rich medium for 6-9 hours and cell morphology (B1), microtubules organization (B2), and nuclear morphology (C, DAPI staining) were observed. Scale bar: 10 μm.

Clb2 is required to enter in mitosis

The *clb2* conditional cells arrested in rich medium with a 2C DNA content, suggesting a post-replicative arrest. As before, to characterize the phenotype of arrested cells, we introduced the *clb2* conditional allele in cells carrying a Cfp-α tubulin fusion. We utilized this new strain, called UMP26, to study the differences between the conditional mutant and wild-type cells in the various growth conditions. The most obvious difference between the conditional strain and wild-type cells growing in liquid medium was the appearance in the mutant culture of a subpopulation of cells in which the bud was elongated to the extent that it was larger than the mother cell. This subpopulation was around 25% of the conditional cells growing in MM-NH_4, and more than 60% in rich medium (Fig. 5A). A detailed analysis of the elongated cells arrested in rich medium, indicated that they carried a single nucleus (Fig. 5C) with a MT cytoskeleton that was consistent with G2 phase (Fig. 5B2).

One plausible interpretation of the above results could be that Clb2 levels are responsible for marking the end of G2 phase and the beginning of mitosis. In the conditional strain growing in restrictive medium, the absence of *clb2* expression resulted in the inability of the cells to enter mitosis and the unlimited growth of the bud. Should this interpretation be correct, an increase in the levels of Clb2 would result in a shorter G2 phase. To examine this hypothesis, we inserted in a wild-type strain an ectopic copy of the *clb2* coding sequence under the control of the P_{crg1} promoter (Brachmann et al., 2001). The expression of this transgene was repressed in glucose-containing medium and induced in arabinose-containing medium, leading to more than 30-fold increase in the levels of Clb2 after 3 hours incubation in complete medium containing arabinose (not shown). In these conditions, overexpression of *clb2* resulted in a dramatic phenotype. The cells lost their typical budding pattern and acquired an elongated shape. Each cell was divided by septation into compartments that each contained a single nucleus (Fig. 6A,B). Each compartment was smaller than a normal *U. maydis* cell (average of less than 10 μm in length, versus 15-20 μm in wild-type cells). FACS analysis indicated that these cells accumulated DNA in genome sized multiples, consistent with a normal DNA replication (Fig. 6B). Our interpretation of such as hyphal-like growth is that the high levels of Clb2 promoted a premature entry into mitosis resulting in the inability to produce the bud and then a division by septation. Because of

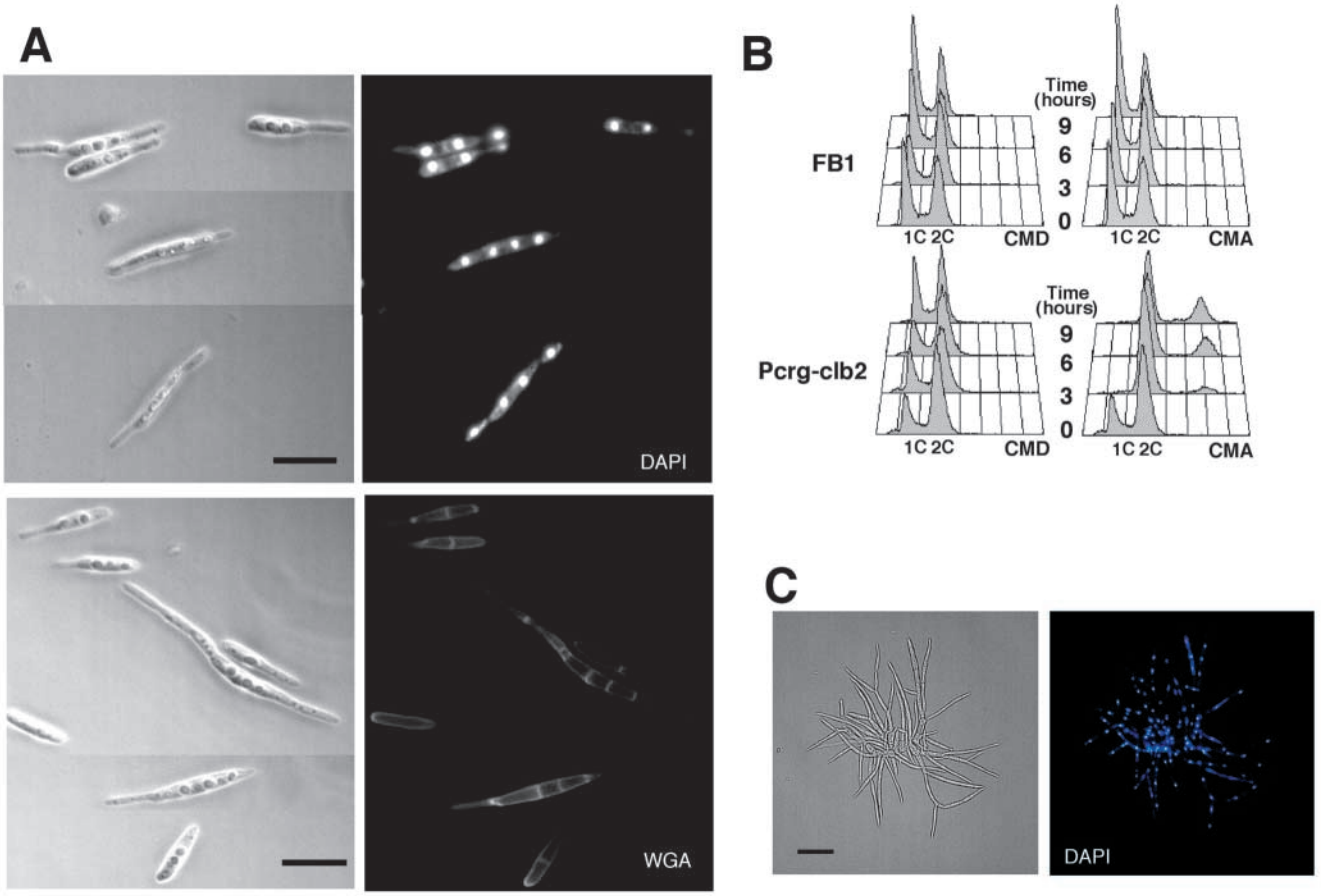

Fig. 6. Consequences of Clb2 overexpression. (A) Cells overexpressing a wild-type copy of Clb2 under the control of the P_{crg1} promoter (TAU52-1 cells) were grown in CM with 2% arabinose for 9 hours and samples were DAPI stained (upper panel), or WGA stained to detect the presence of septa (lower panel). Scale bars: 10 μm. (B) Flow cytometry analysis of wild-type and TAU52-1 (FB1 Pcrg-clb2) cells grown in no induction (CMD) and induction (CMA) conditions. Cells grown in CMD were centrifuged, washed twice in water, and resuspended in the appropriated medium. Samples were taken for FACS analysis at the indicated times. The extra peak in TAU52 cells grown in CMA corresponds to a 4C DNA content. (C) Cell morphology of TAU26 (FB1 P_{hsp70}-clb2) cells growing in liquid CMD medium after 24 hours of incubation. Right panel show DAPI staining. Scale bar: 10 μm.

the dramatic change in morphology observed, we wondered whether the cells were able to support a constitutive high level of *clb2* expression. We have introduced in wild-type cells an ectopic copy of the *clb2* gene cloned under the control of the strong constitutive *hsp70* promoter (which produces around a 40-fold increase in the levels of Clb2; not shown). The resulting strain, TAU26, was viable, but it grew in a filamentous way in liquid medium (Fig. 6C). Taken together, these results indicate a correlation between the bud formation, the length of the G2 phase and the levels of Clb2, supporting the conclusion that the levels of Clb2 could mark the length of G2 and the onset of mitosis.

Overexpression of Clb1 alters chromosomal segregation

In addition to Clb2, the transition from G2 to M also requires the presence of Clb1. To evaluate if Clb1 could also be involved in the control of the length of G2 in *U. maydis*, we examined the consequences of the overexpression of *clb1*. To do this, we introduced into a wild-type strain an ectopic copy of *clb1* under the control of the P_{crg} promoter. In this strain, growth in arabinose-containing medium gave a 50-fold increase in the levels of Clb1 with respect to a wild-type strain (not shown). We observed that such high levels of Clb1 correlated, in liquid cultures, with cells of different sizes that showed altered morphology (Fig. 7A). There were differences in intensity of DAPI staining between cells in these cultures, suggesting differences in DNA content per cell (Fig. 7A). Consistently, FACS analysis of the *clb1*-overexpressing cultures indicated the presence of cells with a DNA content lower than 1C as well as a population of cells with a DNA content higher than 2C (Fig. 7B). Furthermore, *clb1*-overexpressing cells growing in solid medium accumulated phloxine B (a vital stain excluded by living cells) (Fig. 7C), indicating that high levels of Clb1 protein resulted in a loss of viability.

S. cerevisiae cells overexpressing cyclin Clb5 showed an altered chromosome segregation (Sarafan-Vasseur et al., 2002) and mammalian cells overexpressing cyclin E and cyclin B1 also show defects in the segregation of the chromosomes and aneuploidy (Spruck et al., 1999; Yin et al., 2001). Taking into account these reports, a plausible interpretation for our results is that high levels of Clb1 interfere with a normal chromosomal

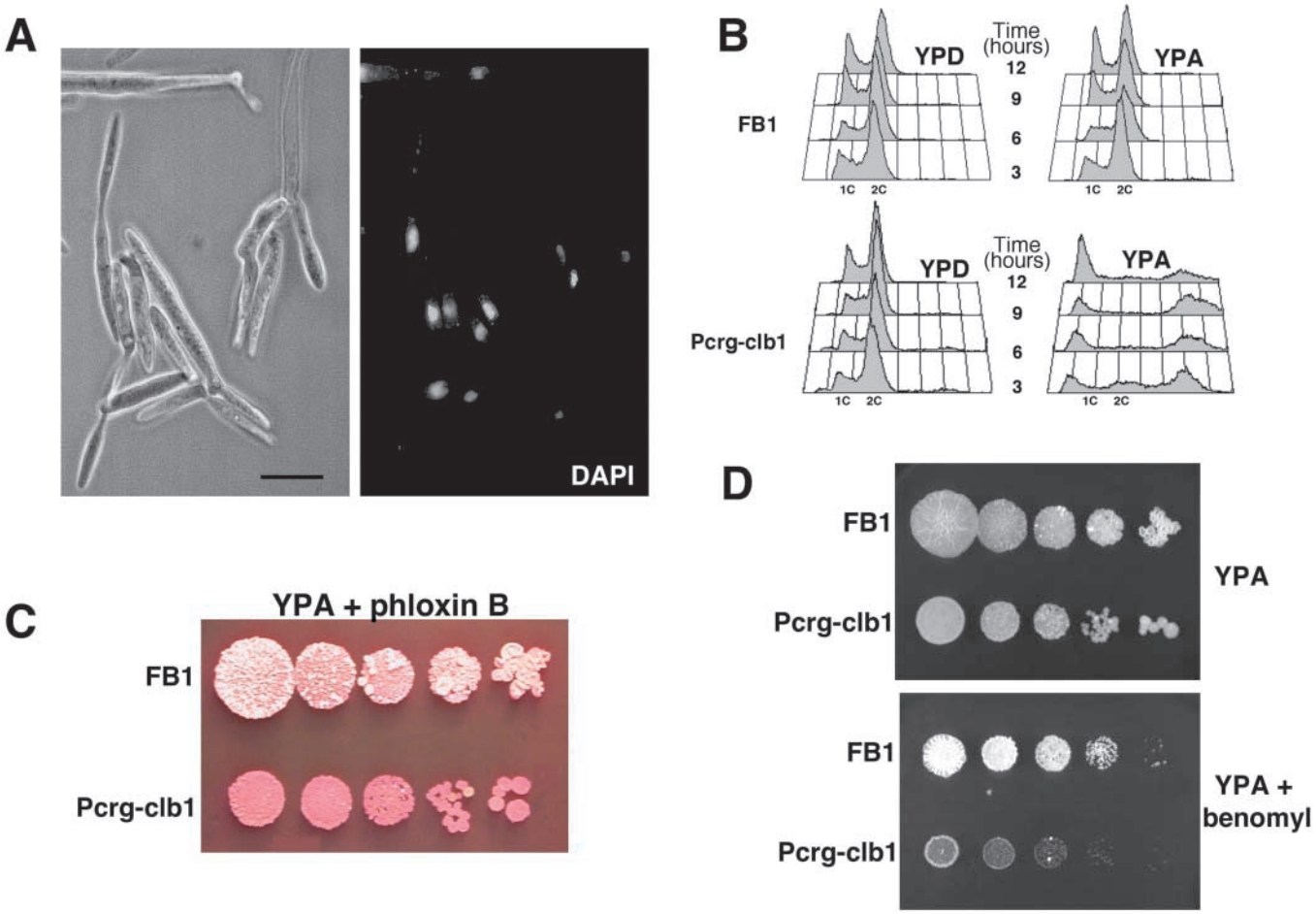

Fig. 7. Consequences of Clb1 overexpression. (A) Cell morphology of TAU36-1 cells growing in YPA (inducing conditions). Observe in the cells stained with DAPI the diverse intensity of fluorescence from various nuclei. Scale bar: 10 μm. (B) Flow cytometry analysis of wild-type (FB1) and TAU36-1 cells grown in no-induction (YPD) and induction (YPA) conditions. Cells grown in YPD were centrifuged, washed twice in water and resuspended in the appropriated medium. Samples were taken for FACS analysis at the indicated times. Note the peaks with DNA content below 1C and above 2C. (C) Serial tenfold dilutions of exponential cultures in YPD of wild-type FB1 and TAU36-1 (FB1 Pcrg-clb1) cells were spotted on induction plates (YPA, YP medium with 2% arabinose) with 5 μg/ml phloxin B and incubated at 28°C for 4 days. Phloxin B accumulates in dead cells and subsequently red colonies are indicative of a loss of viability. (D) Benomyl sensitivity of strain overexpressing Clb1. Serial tenfold dilutions of exponential cultures of FB1 and TAU36-1 cells were spotted on induction plates containing 0.6 μg/ml of benomyl. Plates were incubated at 28°C for 4 days.

segregation, resulting in aneuplody. In *S. pombe*, it has been reported that high levels of Cdc13 resulted in disassembly of microtubules (Yamano et al., 1996). In line with this argument, we found that *U. maydis* cells overexpressing *clb1* were hypersensitive to the microtubule-destabilizing drug benomyl (Fig. 7D). It is plausible to assume that, in *U. maydis*, high levels of Clb1 interfere with the microtubule assembly, providing an explanation for the observed DNA segregation defects.

Expression of indestructible B-cyclins interferes with progression through mitosis in *U. maydis*

The previous results highlight the importance of a strict control in the level of mitotic cyclins in *U. maydis*. One of the ways that eukaryotic cells control the levels of mitotic cyclins is regulated proteolysis mediated by APC/C (Zachariae and Nasmyth, 1999). Cyclin destruction is thought to be mediated by a conserved motif, the destruction box (D-box). *U. maydis* Clb1 has two putative D-boxes as judged by inspection of its sequence (Fig. 8A). One of them is located at the N terminus while the second one is located at the very C terminus. Clb2 has a single putative D-box in its N terminus (Fig. 8A). We constructed truncated versions of both Clb1 and Clb2, in which the various D-boxes were removed (Fig. 8A). These mutant, as well as the full-length versions, were tagged at the C terminus either with the VSV epitope (Clb1 derivatives) or the MYC epitope (Clb2 derivatives) and they were cloned under the control of the P_{crg1}* promoter (Brachmann et al., 2001). This promoter is a less-active version of the P_{crg} promoter that in induction conditions gives only a 10-fold and a 7-fold increase in the levels of Clb1 and Clb2 proteins, respectively, compared to wild-type levels (not shown). The use of this promoter avoids the harmful effects of hyperexpression of *clb1* or *clb2*, reported in previous sections (not shown). We observed that expression of Clb1 derivatives lacking a single D-box had no effect on the ability of the cells to form colonies. However, the

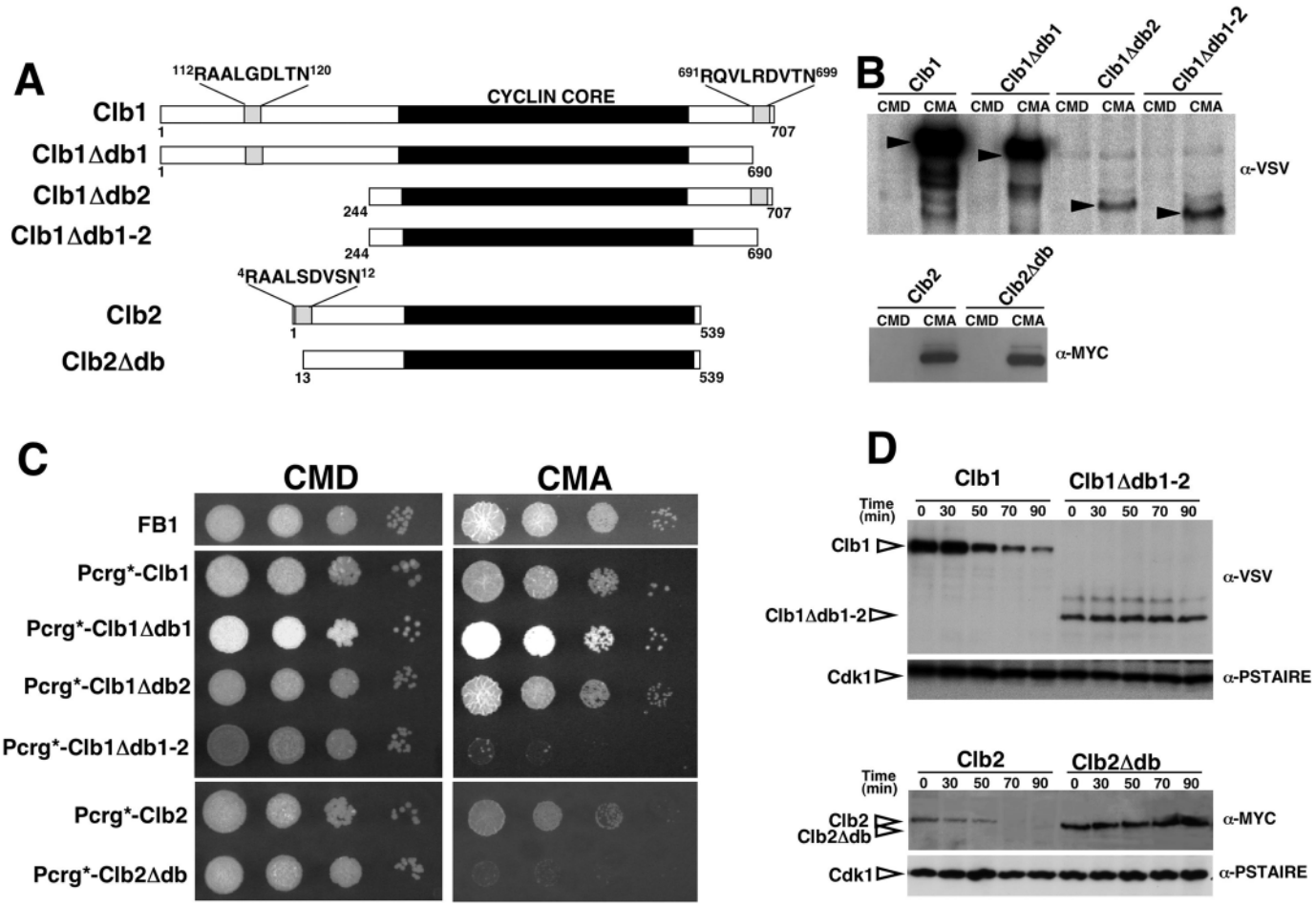

Fig. 8. Clb1 and Clb2 proteins carry functional destruction boxes. (A) Scheme showing the Clb1 and Clb2 proteins, as well the different deletion mutants. The sequences for the destruction boxes are indicated. These constructs were expressed under the control of a less-active version of the Pcrg1 promoter to avoid the problems associated to high cyclin levels (see text for details). (B) Expression levels of Clb1 and Clb2 derivates. Cells were grown in non-induction (complete medium with 2% glucose, CMD) and induction (complete medium with 2% arabinose, CMA) conditions for 6 hours. Whole cell lysates were separated by SDS-PAGE and immunoblotted with anti-VSV (Clb1 western, upper panel) or anti-MYC (Clb2 western, lower panel) antibodies. Similar amount of total extract was loaded per lane. Upper panel: TAU36-2 (Clb1), TAU30 (Clb1Δdb1), TAU45 (Clb1Δdb2) and TAU31 (Clb1Δdb1-2) cells that express VSV-tagged versions of Clb1 and derived proteins. The different level of protein expression could be attributed to a lower translation efficiency in the derivates lacking the N-terminal destruction box. Lower panel: TAU52-2 (Clb2) and TAU53 (Clb2Δdb) cells that express MYC-tagged versions of Clb2 and Clb2Δdb proteins. (C) Serial tenfold dilutions of exponential cultures of FB1 (control), TAU36-2 (P_{crg}*-Clb1), TAU30 (P_{crg}*-Clb1Δdb1), TAU45 (P_{crg}*-Clb1Δdb2), TAU31 (P_{crg}*-Clb1Δdb1-2), TAU52-2 (P_{crg}*-Clb2), and TAU53 (P_{crg}*-Clb2Δdb) strains were spotted on complete medium plates with glucose (CMD) or arabinose (CMA) as sole carbon source. Plates were incubated at 28°C for 3 days. (D) Deletion of D-boxes stabilizes Clb1 and Clb2. TAU36-2, TAU31, TAU52-2 and TAU53 cells were grown for 1 hour in complete medium with 2% arabinose, and then transferred to completed medium with 2% glucose and 100 μg/ml cycloheximide. Samples were taken at the indicated time, and Clb1, Clb2 and Cdk1 levels were analysed by immunoblotting with anti-VSV, anti-MYC and anti-PSTAIRE antibodies respectively.

expression of the truncated *clb1* allele lacking the two D-boxes, *clb1Δdb1-2*, or the expression of the mutant *clb2* allele lacking the D-box, *clb2Δdb*, prevented colony formation (Fig. 8C). This effect is consistent with previous reports of expression of cyclins lacking D-boxes in other yeast systems and it has been attributed to the inability of the mutant cyclins to be degraded by the proteasome, which results in a cell cycle arrest (Ghiara et al., 1991; Surana et al., 1993; Yamano et al., 1996; Yamano et al., 2000). To examine this notion further, first we sought to demonstrate that the *U. maydis* cyclin variants devoid of D-boxes were more stable than their wild-type counterparts. For this, cells carrying either the wild-type or the mutant alleles under the control of the P_{crg1}* promoter were incubated in arabinose-containing medium to allow the expression of the proteins, and after 2 hours of incubation, glucose and cycloheximide were added to shut-off the production of further protein. Samples were removed at different times for western analysis (Fig. 8D). We observed that while Clb1 and Clb2 protein levels declined, the levels of the mutant versions lacking the D-boxes, Clb1Δdb1-2 and Clb2Δdb remain high and almost constant, consistent with more stable proteins.

To assess whether the expression of the stabilized versions of mitotic cyclins induce some specific cell cycle arrest, we introduced the constructions expressing the mutant alleles in a

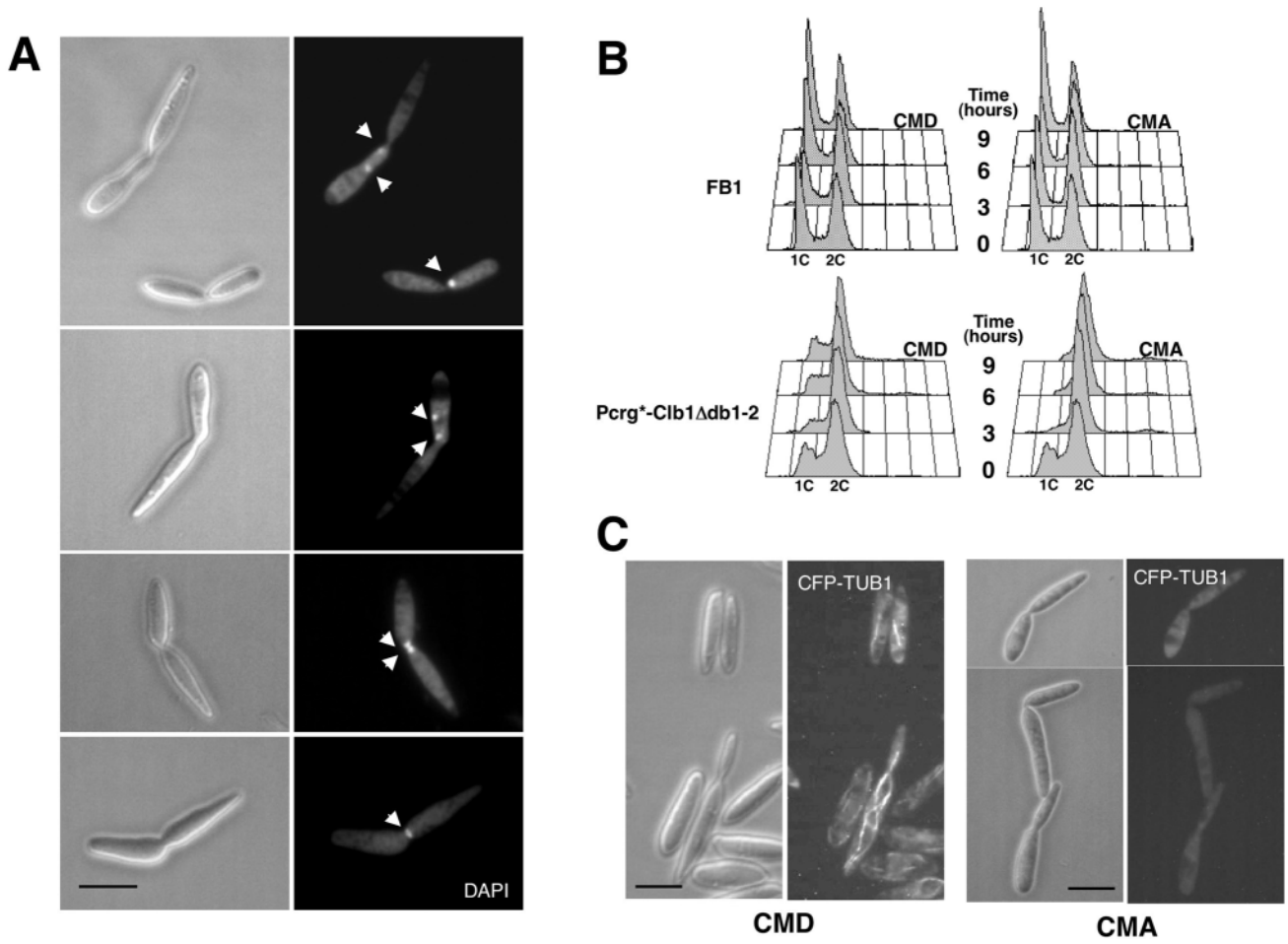

Fig. 9. Effects of the expression of a stable version of Clb1. (A) Cell morphology of TAU57 strain grown in CMA for 9 hours. This strain carries the *clb1Δdb1-2* transgene and a Cfp-tub1 fusion. All cells were arrested with a bud about the size of the mother cell. Three different condensed nucleus morphologies were apparent: a single nucleus near the neck, two nuclei nearby and a nucleus split in two located in the neck (arrows point to nuclei). Scale bar: 10 μm. (B) Cells expressing Clb1Δdb1-2 arrested with a 2C DNA content. Flow cytometry analysis of wild-type FB1 and TAU57 cells grown in no-induction (CMD) and induction (CMA) conditions. Cells grown in CMD were centrifuged, washed twice in water, and resuspended in the appropriated medium. Samples were taken for FACS analysis at the indicated times. (C) Microtubule organization in TAU57 cells growing in non-induction conditions (CMD) and induction conditions (CMA). Observe the absence of microtubule structures in inducing conditions.

strain carrying a Cfp-α tubulin fusion, and the cells growing in induction conditions were analyzed (Figs 9 and 10). Liquid cultures of the strain expressing the *clb1Δdb1-2* allele were composed of budded cells in which three different nuclear morphologies were apparent. Around 60% of the cells carried a single condensed nucleus located near the neck; in 14% of the cells the nucleus appeared split in two halves and located in the neck, and 26% of the cells had two condensed nuclei located not far apart (Fig. 9A). The FACS analysis indicated that all cells had a 2C DNA content (Fig. 9B). Of note, in spite to the fact that cells growing in non-inducing conditions gave a clear microtubule pattern, the incubation in inducing conditions results in cells where no clear microtubule structures were apparent, indicating that the spindles are somewhat unstable in the presence of the mutant *clb1* allele (Fig. 9C). A probable explanation of these phenotypes is that the stabilized mutant version of Clb1 interferes with microtubule assembly, impairing the proper execution of mitosis, and resulting in a cell cycle arrest.

The cells overexpressing the stable *clb2Δdb* allele also arrested with a 2C DNA content (Fig. 10A). However, the morphology was different from cells expressing indestructible Clb1. The arrested cells showed no buds, although they had two well separated nuclei (Fig. 10B). This morphology is similar to the first stages observed when *clb2* is overexpressed (see Fig. 6A), and supports the notion that high levels of Clb2 impaired the budding process (most probably because it induces a premature entry into mitosis). However, in contrast to the overexpression of wild-type *clb2*, no septa were formed between nuclei (Fig. 10C), and microtubule spindles were present (Fig. 10D). Our interpretation of these results is that a failure in Clb2 degradation results in a cell cycle arrest after anaphase, with the cell unable to exit mitosis.

Progression through the infective process requires an accurate control of Clb2 levels

The growth of the fungus inside the plant involves distinct steps

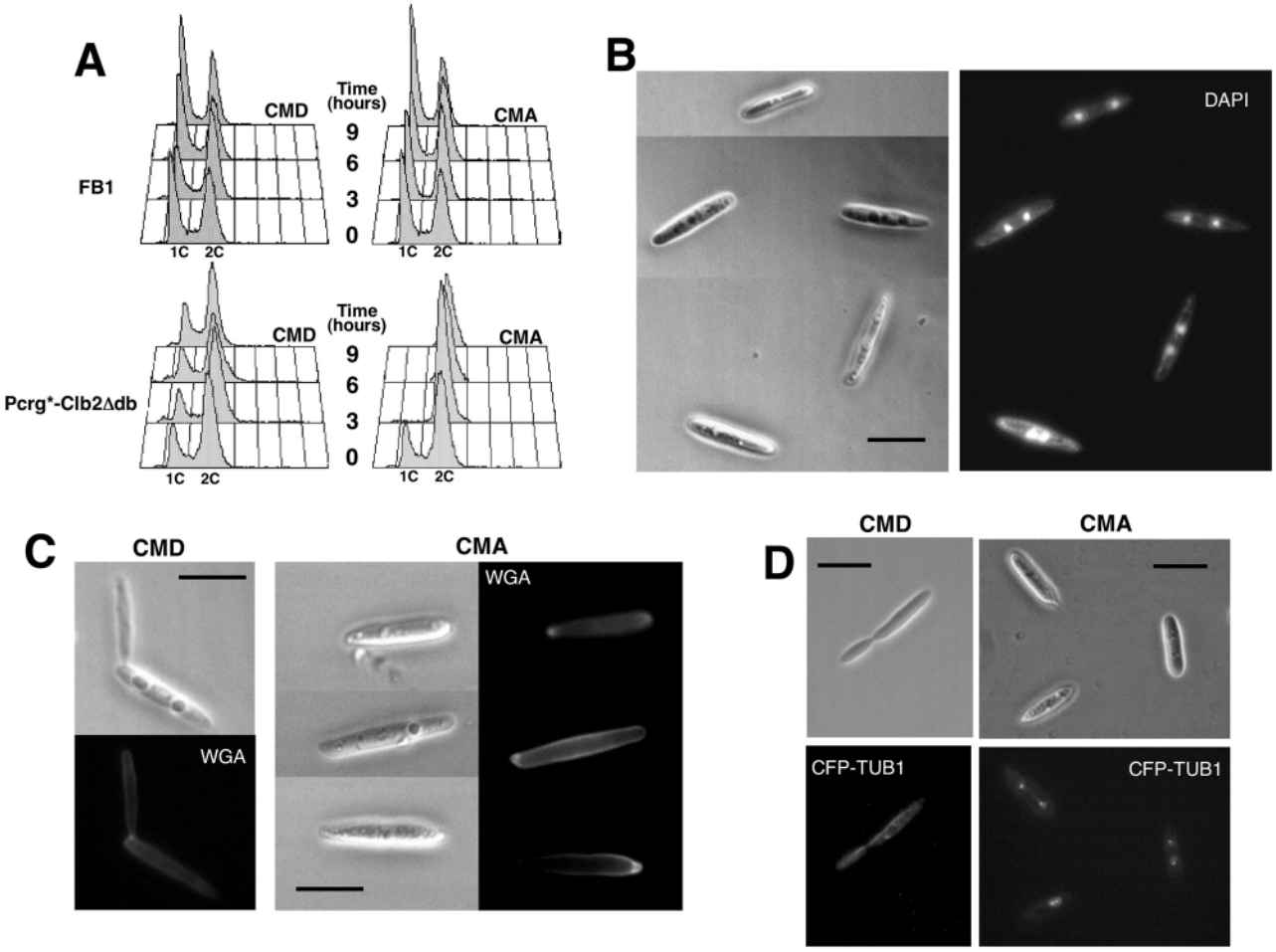

Fig. 10. Effects of the expression of a stable version of Clb2. (A) Cells expressing Clb2Δdb arrested with a 2C DNA content. Flow cytometry analysis of wild-type and TAU58 cells grown in no-induction (CMD) and induction (CMA) conditions. Cells grown in CMD were centrifuged, washed twice in water, and resuspended in the appropriated medium. Samples were taken for FACS analysis at the indicated times. (B) TAU58 cells grown in CMA for 9 hours were stained with DAPI to observe nuclei. (C) TAU58 cells grown for 9 hours in CMD or CMA were stained with WGA to detect the presence of septum in the cells. Note that no septa are apparent in cells growing in CMA. (D) Formation of the mitotic spindle in TAU58 cells treated as before, observed with epifluorescence. Compare the MT pattern in non-induction conditions (CMD) and induction conditions (CMA). Scale bars: 5 μm.

that have been described from microscopic studies (Snetselaar and Mims, 1992; Banuett and Herskowitz, 1996). After fusion of haploid fungal cells and penetration inside the plant, the fungal hypha continues to grow as an unbranched tip cell leaving highly vacuolated portions behind. As the infection progress, the hypha proliferates and septa partition cell compartments, containing a pair of nuclei each. Polar growth continues along the main hypha that begins to form clamp-like structures and branches. Finally, the hyphae undergo fragmentation to release individual cells that will produce the diploid spore (teliospore). During all this process, the host plant responds with the symptoms of infection. Induction of chlorosis is known to be one of the earliest detectable symptoms of *U. maydis* infection (Christenesen, 1963). It is followed by anthocyanin production, a known stress reaction in plants. Finally, the hyperproliferation of plant cells in response to the fungus produces the typical plant tumors. Given the connections between morphogenesis and pathogenesis in *U. maydis*, we were interested in determining whether TAU26 cells that produce constitutively high levels of Clb2 protein and had in a hyphal-like growth (Fig. 6C), were able to cause disease symptoms upon inoculation into corn seedlings. We mixed TAU26 cells with the wild-type compatible haploid strain FB2 and we inoculated plants to test the virulence of the dikaryon produced upon fusion. These inoculations included positive controls of crosses between wild-type strains (FB1 and FB2). As indicated in Table 3, disease symptoms were observed on more than 90% of the plants inoculated with the compatible wild-type strains FB1 and FB2. In contrast, of the 67 plants inoculated with the combination of TAU26 and FB2, 66% showed no observable symptoms and the remaining 44% demonstrated only mild symptoms. The latter plants showed mostly chlorosis emanating from the point of inoculation (Fig. 11A). Interestingly, anthocyanin production was never observed in these plants. To asses at which level TAU26 cells are defective, we first tested the ability of TAU26 cells to mate in charcoal mating plates (Holliday, 1974). The visible white filamentous growth indicative of the dikaryon was slightly

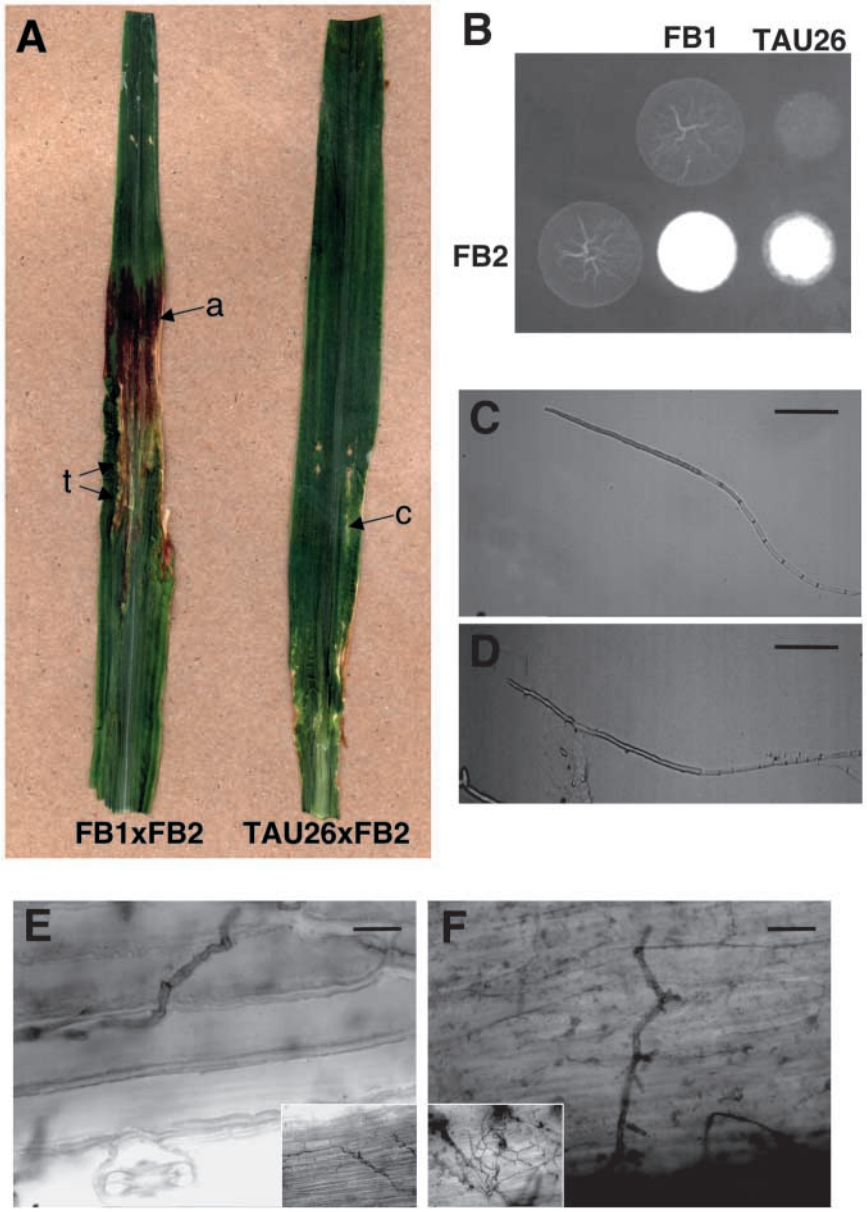

Fig. 11. Influence of high levels of Clb2 in mating and pathogenicity. (A) Disease symptoms on the leaf blades of young maize plants 14 days post inoculation with the strains indicated. Observe the anthocyanin production (arrow a) and small tumors (arrow t) in the wild-type infection and the chlorosis (yellowing of the green tissue of the leaf, arrow c) in the mutant infection. (B) Mating assay of Clb2-overexpressing cells and wild-type strains. The appearance of white filaments indicates formation of dikaryotic hyphae. Note that the mutant cross produced fewer hyphae. (C) Dikaryotic hypha resulting from a wild-type FB1 × FB2 cross. Note the empty compartments to the right of the elongated tip cell. (D) Dikaryotic hypha resulting from a mutant TAU26 × FB2 cross. Note the 'spiky' appearance of the elongated tip cell. (E) Hyphal development of wild-type cells inside the plant tissue. Cross walls separate the long cylindrical cells of hyphe. The inset shows a lower magnification of the filamentous network. (F) Hyphal development of mutant cells inside the plant tissue. These cells appeared to generate incipient branches at a higher frequency than wild-type cells. Scale bars: 50 μm (B,C); 20 μm (E-F).

reduced in the mutant mixture (Fig. 11B). We analyzed the dikaryotic hyphae and observed both in wild-type and mutant mixtures the typical filament where hyphal extension occurs in the absence of mitosis and a fixed volume of cytoplasm migrates forward with the expanding apex, leaving behind an extensively vacuolated and otherwise empty distal cell compartment (Steinberg et al., 1998) (Fig. 11C,D). The only apparent difference is the 'spiky' aspect of the mutant hypha. These results indicate that high levels of Clb2 decreased but did not negate dikaryotic formation. The observation of chlorosis around the site of inoculation indeed suggested that the mutant filaments were capable of growing within the plant tissue. Consequently, symptomatic leaves were sampled, stained and examined microscopically for the presence of the fungus (Fig. 11E,F). Fungal growth was clearly present in maize tissue in plants inoculated with either wild-type or mutant strains. The most obvious difference between mutant and wild-type filaments was the absence of teliospores in mutant mixtures, indicating that mutants failed to complete sexual development. In addition, we noted that the frequency of incipient branches appeared to be higher for filaments in plants infected with the mutant mixture. These results indicate that an extra dose of Clb2 impairs the ability of fungal cells to cause symptoms and progress in the infective cycle.

In order to gain further evidences about the role of Clb2 in virulence, we analyzed the ability to cause disease symptoms

Table 3. Pathogenicity assays

		Chlorosis		Anthocyanin formation		Tumor formation	
Inoculum	Genotype	Total	Percentage	Total	Percentage	Total	Percentage
FB1 × FB2	*a1 b1* × *a2 b2*	51/54	94	50/54	92	49/54	90
TAU26 × FB2	*a1 b1, cbx::*P_{hsp70}*clb2-1* × *a2 b2*	30/67	44	0/67	0	0/67	0
FBD11	*a1a2 b1b2*	56/68	82	54/68	79	54/68	79
UMP21	*a1a2 b1b2 clb1clb1Δ::hph*	60/77	78	58/77	75	55/77	71
UMP32	*a1a2 b1b2 clb2clb2Δ::cbx*	82/97	84	82/97	84	0/97	0

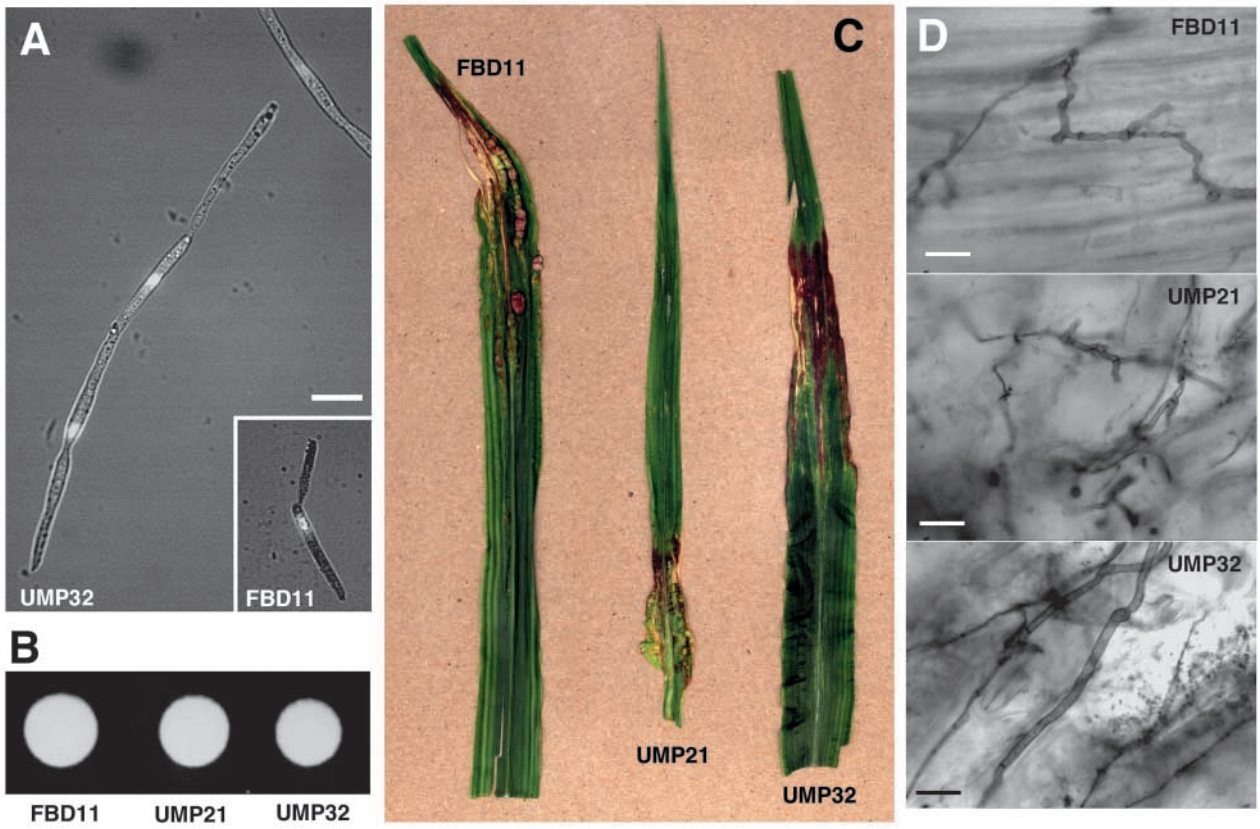

Fig. 12. Infectivity of diploids carrying a single dose of B-cyclin genes. (A) Morphology of a wild-type diploid cell (inset, FBD11 cells at same magnification) and a diploid cell with a single gene dose of *clb2* (UMP32). Cells were grown in CMD to exponential phase and DAPI stained. Scale bar: 10 μm. (B) Charcoal assay of diploid strains heterozygous for mating type. FBD11 is a wild-type strain, UMP21 has a single dose of the *clb1* gene, and UMP32 has a single dose of the *clb2* gene. (C) Disease symptoms on the leaf blades of young maize plants 14 days post inoculation with the strains indicated. Strong anthocyanin production was induced by infection with UMP32 but no tumors were apparent. (D) Hyphal development of wild-type, UMP21 and UMP32 cells inside the plant tissue. Observe that mutant UMP32 cells appeared to have fewer branches and the hyphae look wider the wild-type hyphae. Scale bars: 20 μm.

in plants of a diploid strain carrying a single allele of the *clb2* gene (UMP32). Previously, we have observed that the UMP32 cells were larger than wild-type cells, with elongated buds that sometimes carried more than one nucleus (Fig. 12A). We considered this phenotype as a consequence of the lower levels of Clb2 in these cells, which could result in a delay in mitosis – as we showed in haploid *clb2* conditional strains incubated in restrictive conditions (Fig. 5B1). This haploinsufficiency was specific for *clb2*, since a diploid strain carrying a single copy of the *clb1* gene (UMP21), had a wild-type phenotype (not shown). First, we have tested for colony morphology on charcoal mating plates. The filamentous growth phenotype that arises from mating between haploid strains is also displayed by diploid strains of *U. maydis* that are heterozygous for both the *a* and *b* mating-type loci. As shown in Fig. 12B, filamentous colonies are formed by the wild-type diploid strain FBD11 as well as by the mutant diploid strains UMP21 and UMP32, indicating that half a dose of *clb1* or *clb2* is not detrimental at this step. Second, we inoculated plants with cultures of FBD11, UMP21 and UMP32 cells. As shown in Table 3, the strain carrying a single *clb1* allele was as virulent as the diploid wild-type control. In contrast, we found that diploid cells defective in one *clb2* allele were capable of causing chlorosis and anthocyanin production but tumors were never observed. Interestingly, the anthocyanin production was even stronger in plants infected with the UMP32 strain that in plants infected with FBD11 strain. We also studied the fungal growth inside the plant tissue. The hyphae of the UMP21 cells were similar to those of wild-type cells. In contrast, several differences were observed in the UMP32 hyphae: they were wider, less septate and they showed fewer branches than wild-type hyphae. No teliospores were present in the UMP32-infected plants (not shown).

Taken together, these results strongly suggest that Clb2 levels in *U. maydis* must be accurately controlled during the infection process, and that inability to do so blocks the complete sexual development.

Discussion

In the current study, we have characterized the genes encoding the CDK catalytic subunit, Cdk1 and two regulatory subunits, the B-type cyclins Clb1 and Clb2 in the phytopathogenic fungus *U. maydis*. The *cdk1* gene is essential and encodes a protein with high sequence similarity to other members of the Cdc2 protein family. The *clb1* and *clb2* genes encode B-type cyclins. Analysis of their coding sequences indicates typical sequence signatures of B-type cyclins. Both proteins interact

with Cdk1 and their levels change in cells arrested at different cell cycle stages. A search performed in the *U. maydis* genome indicated that no other B-type cyclins were present (http://www.broad.mit.edu/annotation/fungi/ustilago_maydis/index.html). This situation is in contrast to other well-know fungi such as *S. cerevisiae* or *S. pombe*, where there is a certain degree of redundancy in cyclin content and in the roles these cyclins play. However, the situation in *U. maydis* is likely to be more general. For instance, the human pathogen *Candida albicans* appears to have only two B-type cyclin (J. Berman, personal communication).

Clb1 plays an essential role in the cell and is required to perform the G1 to S and the G2 to M transitions. In *S. pombe*, the G1 to S and G2 to M transitions are performed by Cig2 and Cdc13, respectively (Booher and Beach, 1987; Hagan et al., 1988; Bueno and Russell, 1993; Connolly and Beach, 1994), although in *S. pombe* cells deleted for the *cig2* gene, Cdc13 substitutes for Cig2 to bring about the G1 to S transition (Fisher and Nurse, 1996; Mondesert et al., 1996). Interestingly, in a dendrogram analysis of B-type cyclins from different fungi, *U. maydis* Clb1 was clustered along with the Cig2 and Cdc13 cyclins. How does Cdk1-Clb1 kinase first promote G1 to S transition early in the cell cycle and then prevent the reinitiation during G2? A hypothesis that seems reasonable is to assume that additional elements, specific for each transition, modify the scope of target molecules of this complex. Clb2 appears to be specific for G2/M transition and it seems to be a rate-limiting regulator for entry into mitosis. Cells carrying a conditional *clb2* allele growing in restrictive conditions were arrested in G2 phase with an elongated bud displaying an active polarized growth. In contrast, high levels of Clb2 expression resulted in short cells that divided by septation, producing a hyphal-like growth. In *U. maydis*, the G2 phase is characterized by polar growth that results in the elongation of the bud. It could well be that the levels of Clb2 mark the length of G2 and then the size of the bud. This could be related with a G2/M size control operating through the levels of Cdk1-Clb2. The postulated role of Clb2 is reminiscent of the roles proposed for cyclin A in humans (Furuno et al., 1999) and cyclin B2 in plants (Weingartner et al., 2003) as promoters of mitosis. In human cells it has been demonstrated that cyclin A/CDK2 activity is a rate-limiting component for entry into mitosis because exogenous active cyclin A/CDK2 will drive cells prematurely into mitosis (Furuno et al., 1999). In plants, induction of ectopic cyclin B2 expression drives cells to enter mitosis earlier, causing developmental abnormalities in transgenic plants (Weingartner et al., 2003). We do not yet have a clear view of how Clb1 and Clb2 cooperate in the G2/M transition. For instance, Clb2 could regulate Clb1 activity in G2 or both cyclins could act in different targets to jointly induce mitosis. Because of the different phenotypes observed in cells overexpressing either *clb1* or *clb2*, we favored the latter hypothesis.

The Clb1 and Clb2 mitotic cyclins contain typical destruction boxes. By deletion analysis we demonstrated that they are functional. The inability to down-regulate the cyclin levels properly resulted in cell cycle arrest. We have shown that cells expressing a mutant version of Clb2 lacking the destruction box are unable to exit mitosis and arrest after anaphase, as has been demonstrated with stabilized versions of mitotic cyclins in other organisms (Surana et al., 1993; Yamano et al., 2000). The expression of the *clb1Δdb1-2* allele, in contrast, produces a cell cycle arrest at some point between metaphase and anaphase, with cells unable to assemble spindles. We cannot determine whether the inability to proceed through mitosis in these cells is a consequence of the microtubule disassembly or whether the cell cycle arrest promotes such disorganization. However, we favored the first explanation. In *S. pombe* it has been reported that high levels of Cdc13 resulted in disassembly of microtubules (Yamano et al., 1996). Furthermore, consistent with the idea that in *U. maydis* high levels of Clb1 interfere with microtubule assembly, we showed that overexpression of *clb1* resulted in cells that were hypersensitive to the microtubule inhibitor benomyl and had anomalous DNA content. A general feature observed in basidiomycete yeast is the presence of an extensive microtubule network in G2 that disassembles prior to mitosis and then forms the mitotic spindle (Steinberg et al., 2001; Kopecká et al., 2001; Banuett and Herskowitz, 2002). We entertained the idea that an initial step to enter in mitosis could be the premitotic activation of Cdk1-Clb1 that could induce the disassembly of the cytoplasmic microtubule network. Such a role of Cdk1-Clb1 in the induction of mitosis could help to explain the fact that in *clb1* conditional cells incubated in restrictive conditions, when the bud is present, the nucleus migrates to the daughter compartment (a pre-mitosis step) but the microtubule cytoskeleton still keeps a typical G2 appearance. In this line of argument, it could be possible that the posterior inhibition of Clb1-Cdk1 activity (i.e. by proteolysis of Clb1) allows the assembly of microtubules to form the mitotic spindles. If this is the case, the presence of an indestructible version of Clb1 could preclude the spindle assembly, as we observed.

Taking all the above conclusions into account we suggest a working model of how the cell cycle proceeds in *U. maydis*. In our model, the G1 to S transition requires Cdk1-Clb1 activity. Whether Cdk1-Clb1 is the only requirement or additional elements (i.e. G1 cyclins) are needed to induce the G1/S transition remains to be clarified. Once DNA replication ends, the formation of the bud marks the beginning of G2. Once, the proper bud size is reached, mitosis is induced. The onset of mitosis requires both Cdk1-Clb1 and Cdk1-Clb2, with a specific role of Cdk1-Clb2 determining the length of G2 phase. Once mitosis is induced, cyclins must be degraded, most probably by APC/C. Based upon the results with stabilized cyclins, we postulate that Clb1 should be removed earlier in mitosis, whilst Clb2 should be removed later. We believe that this working model will provide a basis where additional regulatory elements, like APC/C, CDK inhibitory elements and other additional cell cycle regulators could be added in future. Isolation of specific cell cycle termosensitive mutants and studies with synchronous cultures could help us come to a better understanding of these issues.

In *Ustilago maydis*, an accurate control of cell cycle must be required not only in cells growing in vegetative conditions, but also during the infection process. Hyphal growth within the plant is a dynamic process that requires several stages of differentiation and then, pathogenesis, morphogenesis and cell cycle are predicted to be connected in this fungus. Our findings strongly suggest that progression through the different steps in infection requires a careful control of cell cycle. We had found that infection of a plant by fungal cells

with high levels of Clb2 produces only symptoms of chlorosis, while infection with fungal cells carrying half a dose of Clb2 induces the production of anthocyanin by the plant, but tumor production does not occur. We believe that the accurate control of cyclin levels could be required not only to adjust the fungal morphogenesis inside the plant, but also to properly induce the developmental program that allows other processes such as plant-fungus signaling or biosynthesis and release of tumor inducing chemicals, for instance. Interestingly, the phenotypes found in *clb2* mutants were reminiscent of mutants defective in genes involved in signaling in *U. maydis*. For instance, in mutants defective in *ubc1*, which encodes the regulatory subunit of PKA, or in *ukb1*, which encodes a serine/threonine protein kinase with a role in budding and filamentous growth, the development of the fungus is somehow interrupted in the shift from colonization and ramification to tumor formation (Gold et al., 1997; Abramovitch et al., 2002). It has been proposed that the defect of these signaling mutants in tumor induction could be related to an inability to sense or respond to host stimuli that are required for the production of the signal or signals that *U. maydis* emits to trigger tumor formation (Abramovitch et al., 2002). It is tempting to speculate that inability to adapt the cell cycle in response to plant signals impairs the execution of the fungal developmental program that induces the tumor formation in the plant. It follows from this speculation that cell cycle control must be an important downstream target in the fungus-plant interaction. Future experiments will address these connections.

We wish to thank Dr Peter Schreier, for BLAST analysis of the *U. maydis* genome and critical reading of the manuscript. Prof. David W. Holloman is thanked for a critical reading and improvement of the manuscript. We thank Prof. Judith Berman for critical reading of the manuscript. The help of Prof. Jaime Correa-Bordes and Dr Miguel Angel Blanco with the use of Suc1 to isolate CDK is also thanked. The Bayer CropScience AG is acknowledged for providing the genomic sequence of *Umclb2*. We are grateful to Prof. R. Kahmann and laboratory members for generous supply of reagents and support. This work was supported by Grant BIO99-0906 and BIO2002-03503 from MCyT to J.P.-M. and Grant SP1111 from DFG to GS. This manuscript is dedicated to the memory of Ira Herskowitz.

References

Abramovitch, R. B., Yang, G. and Kronstad, J. W. (2002). The *ukb1* gene encodes a putative protein kinase required for bud site selection and pathogenicity in *Ustilago maydis*. *Fungal Genet. Biol.* **37**, 98-108.

Banks, G. R., Shelton, P. A., Kanuga, N., Holden, D. W. and Spanos, A. (1993). The *Ustilago maydis nar1* gene encoding nitrate reductase activity: sequence and transcriptional regulation. *Gene* **131**, 69-78.

Banuett, F. (1995). Genetics of *Ustilago maydis*, a fungal pathogen that induces tumors in maize. *Annu. Rev. Genetics* **29**, 179-208.

Banuett, F. and Herskowitz, I. (1989). Different *a* alleles are necessary for maintenance of filamentous growth but not for meiosis. *Proc. Natl. Acad. Sci. USA* **86**, 5878-5882.

Banuett, F. and Herskowitz, I. (1996). Discrete developmental stages during teliospore formation in the corn smut fungus, *Ustilago maydis*. *Development* **122**, 2965-2976.

Banuett, F. and Herskowitz, I. (2002). Bud morphogenesis and the actin and microtubule cytoskeletons during budding in the corn smut fungus, *Ustilago maydis*. *Fungal Genet. Biol.* **37**, 149-170.

Beach, D., Durkacz, B. and Nurse, P. (1982). Functionally homologous cell cycle genes in budding and fission yeast. *Nature* **300**, 706-709.

Booher, R. and Beach, D. (1987). Interaction between *cdc13*$^{+}$ and *cdc2*$^{+}$ in the control of mitosis in fission yeast; dissociation of the G1 and G2 roles of the *cdc2*$^{+}$ protein kinase. *EMBO J.* **6**, 3441-3447.

Bottin, A., Kämper, J. and Kahmann, R. (1996). Isolation of a carbon source-regulated gene from *Ustilago maydis*. *Mol. Gen. Genet.* **253**, 342-352.

Bölker, M., Böhnert, H. U., Braun, K. H., Görl, J. and Kahmann, R. (1995). Tagging pathogenicity genes in *Ustilago maydis* by restriction enzyme-mediated integration (REMI). *Mol. Gen. Genet.* **248**, 547-552.

Brachmann, A., Weinzierl, G., Kämper, J. and Kahmann, R. (2001). Identification of genes in the bW/bE regulatory cascade in *Ustilago maydis*. *Mol. Microbiol.* **42**, 1047-1063.

Brachmann, A., Schirawski, J., Müller, P. and Kahmann, R. (2003). An unusual MAP kinase is required for efficient penetration of the plant surface by *Ustilago maydis*. *EMBO J.* **22**, 2199-2210.

Bueno, A. and Russell, P. (1993). Two fission yeast B-type cyclins, Cig2 and Cdc13, have different functions in mitosis. *Mol. Cell. Biol.* **13**, 2286-2297.

Christensen, J. J. (1963). Corn smut caused by *Ustilago maydis*. Monnograph no. 2. *Amer. Phytopath. Society*.

Connolly, T. and Beach, D. (1994). Interaction between the Cig1 and Cig2 B-type cyclins in the fission yeast cell cycle. *Mol. Cell. Biol.* **14,** 768-776.

Davey, J. (1998). Fusion of a fission yeast. *Yeast* **14**, 1529-1566.

Ducommun, B. and Beach, D. (1990). A versatile microtiter assay for the universal cdc2 cell cycle regulator. *Anal. Biochem.* **187**, 94-97.

Fisher, D. L. and Nurse, P. (1995). Cyclins of the fission yeast *Schizosaccharomyces pombe*. *Semin. Cell Biol.* **6**, 73-78.

Fisher, D. L. and Nurse, P. (1996). A single fission yeast mitotic cyclin B p34^{cdc2} kinase promotes both S-phase and mitosis in the absence of G1 cyclins. *EMBO J.* **15**, 850-860.

Fitch, I., Dahmann, C., Surana, U., Amon, A., Nasmyth, K., Goetsch, L., Byers, B. and Futcher, B. (1992). Characterization of four B-type cyclin genes of the budding yeast *Saccharomyces cerevisiae*. *Mol. Biol. Cell* **3**, 805-818.

Fleig, U. N. and Gould, K. L. (1991). Regulation of Cdc2 activity in *Schizosaccharomyces pombe*: the role of phosphorylation. *Semin. Cell Biol.* **2**, 195-204.

Furuno, N., den Elzen, N. and Pines, J. (1999). Human cyclin A is required for mitosis until mid prophase. *J. Cell Biol.* **147**, 295-306.

García-Muse, T., Steinberg, G. and Pérez-Martín, J. (2003). Pheromone-induced G2 arrest in the phytopathogenic fungus *Ustilago maydis*. *Euk. Cell* **2**, 494-500.

Garrido, E. and Pérez-Martín, J. (2003). The *crk1* gene encodes an Ime2-related protein that is required for morphogenesis in the plant pathogen *Ustilago maydis*. *Mol. Microbiol.* **47**, 729-743.

Ghiara, J. B., Richardson, H. E., Sugimoto, K., Henze, M., Lew, D. J., Wittenberg, C. and Reed, S. J. (1991). A B cyclin homolog in *S. cerevisiae*: Chronic activation of the Cdc28 protein kinase by cyclin prevents exit from mitosis. *Cell* **65**, 163-174.

Gillissen, B., Bergemann, J., Sandmann, C., Schrör, B., Bölker, M. and Kahmann, R. (1992). A two-component regulatory system for self/non-self recognition in *Ustilago maydis*. *Cell* **68**, 647-657.

Glotzer, M., Murray, A. W. and Krischner, M. W. (1991). Cyclin is degraded by the ubiquitin pathway. *Nature* **349**, 132-138.

Gold, S. E., Brogdon, S. E., Mayorga, M. E. and Kronstad, J. W. (1997). The *Ustilago maydis* regulatory subunit of a cAMP-dependent protein kinase is required for gall formation in maize. *Plant Cell* **9**, 1585-1594.

Hagan, I., Hayles, J. and Nurse, P. (1988). Cloning and sequencing of the cyclin-related *cdc13*$^{+}$ gene and a cytological study of its role in fission yeast mitosis. *J. Cell Sci.* **91**, 587-595.

Holliday, R. (1965). Induced mitotic crossing-over in relation to genetic replication in synchronously dividing cells of *Ustilago maydis*. *Genet. Res.* **6**, 104-120.

Holliday, R. (1974). *Ustilago maydis*. In *Handbook of Genetics* (ed. R. C. King). Plenum Press, New York, USA.

Jacobs, C. W., Mattichak, S. J. and Knowles, J. F. (1994). Budding patterns during the cell cycle of the maize smut pathogen *Ustilago maydis*. *Can J. Bot.* **72**, 1675-1680.

Jeffrey, P. D., Russo, A. A., Polyak, K., Gibbs, E., Hurwitz, J., Massage, J. and Pavletich, N. P. (1995). Mechanism of CDK activation revealed by the structure of a cyclin A-CDK2 complex. *Nature* **376**, 313-320.

Kahmann, R., Steinberg, G., Basse, C., Feldbrügge, M. and Kämper, J. (2000). *Ustilago maydis*, the causative agent of corn smut disease. In *Fungal Pathology* (ed. J. W. Kronstad). Kluwer Academic Publishers, Dodrecht, The Netherlands.

Kopecká, M., Gabriel, M., Takeo, K., Yamaguchi, M., Svoboda, A.,

Ohkusu, M., Hata, K. and Yoshida, S. (2001). Microtubules and actin cytoskeleton in *Cryptococcus neoformans* compared with ascomycetous budding and fission yeasts. *Eur. J. Cell Biol.* **80**, 303-311.

Krylov, D. M., Nasmyth, K. and Koonin, E. V. (2003). Evolution of eukaryotic cell cycle regulation: stepwise addition of regulatory kinases and late advent of the CDKs. *Curr. Biol.* **13**, 173-177.

Liao, S. M., Zhang, J., Jeffery, D. A., Koleske, A. J., Thompson, C. M., Chao, D. M., Viljoen, M., van Vuuren, H. J. and Young, R. A. (1995). A kinase-cyclin pair in the RNA polymerase II holoenzyme. *Nature* **374**, 193-196.

Mondesert, O., McGowan, C. H. and Russell, P. (1996). Cig2, a B-type cyclin, promotes the onset of S in *Schizosaccharomyces pombe*. *Mol. Cell. Biol.* **16**, 1527-1533.

Nasmyth, K. (1993). Control of the yeast cell cycle by the CDC28 protein kinase. *Curr. Biol.* **5**, 166-179.

Nigg, E. A. (1995). Cyclin-dependent protein kinases: key regulators of the eukaryotic cell cycle. *BioEssays* **17**, 471-480.

O'Donnell, K. L. and McLaughlin, D. J. (1984). Postmeiotic mitosis, basidiospore development, and septation in *Ustilago maydis*. *Mycologia* **76**, 486-502.

Pines, J. and Hunter, T. (1991). Cyclin-dependent kinases: a new cell cycle motif? *Trends Cell Biol.* **1**, 117-121.

Pringle, J. R. and Hartwell, L. H. (1981). The *Saccharomyces* cell cycle. In *The Molecular Biology of the Yeast* Saccharomyces (ed. J. N. Strathern, E. W. Jones and J. R. Broach), pp 97-142. New York: Cold Spring Harbor Laboratory.

Richardson, H., Lew, D. J., Henze,M., Sugimoto, K. and Reed, S. I. (1992). Cyclin-B homologs in *Saccharomyces cerevisiae* function in S phase and in G2. *Genes Dev.* **6**, 2021-2034.

Sarafan-Vasseur, N., Lamy, A., Bourguignon, J., Le Pessot, F., Hieter, P., Sesboüé, R., Bastard, C., Frébourg, T. and Flaman, J. M. (2002). Overexpression of B-type cyclins alters chromosomal segregation. *Oncogene* **21**, 2051-2057.

Siebert, P. D., Chenchik, A., Kellog, D. E., Lukyanov, K. A. and Lukyanov, S. A. (1995). An improved method for walking in uncloned genomic DNA. *Nucleic Acid Res.* **23**, 1087-1088.

Snetselaar, K. M. (1993). Microscopic observation of *Ustilago maydis* mating interactions. *Exp. Mycol.* **17**, 345-355.

Snetselaar, K. M. and Mims, C. W. (1992). Sporidial fusion and infection of maize seedlings by the smut fungus *Ustilago maydis*. *Mycologia* **84**, 193-203.

Snetselaar, K. M. and McCann, M. P. (1997). Using microdensitometry to correlate cell morphology with the nuclear cycle in *Ustilago maydis*. *Mycologia* **89**, 689-697.

Sprague, G. F. and Thorner, J. W. (1992). Pheromone response and signal transduction during the mating process of *Saccharomyces cerevisiae*. In *The Molecular and Cellular Biology of the Yeast* Saccharomyces*: Gene Expression* (ed. J. R. Broach, J. R. Pringle and E. W. Jones). New York: Cold Spring Harbor Laboratory Press, Cold Spring Harbor, USA.

Spruck, C. H., Won, K. A. and Reed, S. I. (1999). Deregulated cyclin E induces chromosome instability. *Nature* **401**, 297-300.

Steinberg, G., Schliwa, M., Lehmler, C., Bölker, M., Kahmann, R. and McIntosh, J. R. (1998). Kinesin from the plant pathogenic fungus *Ustilago maydis* is involved in vacuole formation and cytoplasmic migration. *J. Cell Sci.* **111**, 2235-2246.

Steinberg, G., Wedlich-Söldner, R., Brill, M. and Schulz, I. (2001). Microtubules in the fungal pathogen *Ustilago maydis* are highly dynamic and determine cell polarity. *J. Cell Sci.* **114**, 609-622.

Surana, U., Amon, A., Dowzer, C., McGrew, J., Byers, B. and Nasmyth, K. (1993). Destruction of the Cdc28/Clb mitotic kinase is not required for the metaphase to anaphase transition in budding yeast. *EMBO J.* **12**, 1969-1978.

Thompson, J. D., Gibson T. J., Plewniak, F., Jeanmougin, F. and Higgins, D. G. (1997). The CLUSTAL_X windows interface: flexible strategies for multiple alignment aided by quality analysis tools. *Nucleic Acid Res.* **25**, 4876-4882.

Tsukuda, T., Carleton, S., Fotheringham, S. and Holloman, W. K. (1988). Isolation and characterization of an autonomously replicating sequence from *Ustilago maydis*. *Mol. Cell. Biol.* **8**, 3703-3709.

Wedlich-Söldner, R., Bölker, M., Kahmann, R. and Steinberg, G. (2000). A putative endosomal t-SNARE links exo- and endocytosis in the phytopathogenic fungus *Ustilago maydis*. *EMBO J.* **19**, 1974-1986.

Wedlich-Söldner, R., Straube, A., Friedrich, M. W. and Steinberg, G. (2002). A balance of KIF1A-like kinesin and dynein organizes early endosomes in the fungus *Ustilago maydis*. *EMBO J.* **21**, 2946-2957.

Weingartner, M., Pelayo, H. R., Binarova, P., Zwerger, K., Melikant, B., de la Torre, C., Heberle-Bors, E. and Bögre, L. (2003). A plant cyclin B2 is degraded early in mitosis and its ectopic expression shortens G2-phase and alleviates the DNA-damage checkpoint. *J. Cell Sci.* **116**, 487-498.

Yamano, H., Gannon, J. and Hunt, T. (1996). The role of proteolysis in cell cycle progression in *Schizosaccharomyces pombe*. *EMBO J.* **15**, 5268-5279.

Yamano, H., Kitamura, K., Kominami, K. I., Lehmann, A., Katayama, S., Hunt, T. and Toda, T. (2000). The spike of S phase cyclin Cig2 expression at the G1-S border in fission yeast requires both APC and SCF ubiquitin ligases. *Mol. Cell* **6**, 1377-1387.

Yin, X. Y., Grove, L., Datta, N. S. Katula, K., Long, M. W. and Prochownik, E. V. (2001). Inverse regulation of cyclin B1 by c-Myc and p53 and induction of tetraploidy by cyclin B1 overexpression. *Cancer Res.* **61**, 6487-6493.

Zachariae, W. and Nasmyth, K. (1999). Whose end is destruction: Cell division and the anaphase-promoting complex. *Genes Dev.* **13**, 2039-2058.